

REPORT DOCUMENTATION PAGE			Form Approved OMB NO. 0704-0188	
Public Reporting burden for this collection of information is estimated to average 1 hour per response, including the time for reviewing instructions, searching existing data sources, gathering and maintaining the data needed, and completing and reviewing the collection of information. Send comment regarding this burden estimates or any other aspect of this collection of information, including suggestions for reducing this burden, to Washington Headquarters Services, Directorate for information Operations and Reports, 1215 Jefferson Davis Highway, Suite 1204, Arlington, VA 22202-4302, and to the Office of Management and Budget, Paperwork Reduction Project (0704-0188,) Washington, DC 20503.				
1. AGENCY USE ONLY (Leave Blank)		2. REPORT DATE January 15, 2009		3. REPORT TYPE AND DATES COVERED STTR Phase I Final Report
4. TITLE AND SUBTITLE Liquid Metal Anode for JP-8 Fuel Cell			5. FUNDING NUMBERS	
6. AUTHOR(S) Dr. Thomas Tao CellTech Power, PI, Dr. Ralph White USC, Stephen Klotz Lockheed Martin MS3				
7. PERFORMING ORGANIZATION NAME(S) AND ADDRESS(ES) CellTech Power LLC 131 Flanders Rd., Westborough, MA, University of South Carolina 901 Sumter St Byrnes Bldg. Columbia, SC 29208, Lockheed Martin			8. PERFORMING ORGANIZATION REPORT NUMBER 702 Final	
9. SPONSORING / MONITORING AGENCY NAME(S) AND ADDRESS(ES) U. S. Army Research Office P.O. Box 12211 Research Triangle Park, NC 27709-2211			10. SPONSORING / MONITORING AGENCY REPORT NUMBER W911NF-08-C-0075	
11. SUPPLEMENTARY NOTES The views, opinions and/or findings contained in this report are those of the author(s) and should not be construed as an official Department of the Army position, policy or decision, unless so designated by other documentation.				
12 a. DISTRIBUTION / AVAILABILITY STATEMENT Approved for public release; distribution unlimited.			12 b. DISTRIBUTION CODE	
13. ABSTRACT (Maximum 200 words) Report developed under STTR contract W911NF-08-C-0075 for topic A08-T007. JP-8 is a high-energy density liquid fuel available to the soldier, but its electrochemical oxidation in a fuel cell is problematic. The purpose of this effort is to advance the development of a liquid metal based fuel cell operating directly on JP-8 for application in a field portable battery charger. During Phase 1 an evaluation was performed of a range of liquid metal anodes capable of oxidizing JP-8, including several p-orbital metals. Liquid tin selected as the only anode material that has demonstrated sustainable electrochemical oxidation of JP-8. The relevant physio-chemical governing parameters were defined for fuel oxidation by liquid tin. One-dimensional steady state and transient simulation models of the fuel cell were created. The models identified optimization pathways including reduced cathode polarization and lower electrolyte polarization. Finally, a conceptual design was developed for a complete 500 watt battery charger operating on JP-8. Based on mission needs analysis, a systems requirement matrix was developed. Systems engineering tasks included a system level thermodynamic analysis and development of conceptual drawings of the overall system. Suggested tasks for Phase 2 include the construction of a direct JP-8 stack for testing and demonstration.				
14. SUBJECT TERMS STTR Report: Generator, Battery Charger, JP-8, Fuel Cell, Direct Carbon, Portable Power			15. NUMBER OF PAGES 43	
			16. PRICE CODE	
17. SECURITY CLASSIFICATION OR REPORT UNCLASSIFIED	18. SECURITY CLASSIFICATION ON THIS PAGE UNCLASSIFIED	19. SECURITY CLASSIFICATION OF ABSTRACT UNCLASSIFIED	20. LIMITATION OF ABSTRACT UL	

NSN 7540-01-280-5500

Standard Form 298 (Rev.2-89)
Prescribed by ANSI Std. Z39-18
298-102

Enclosure 1

Contents

1	Mission need for small JP-8 generators	4
1.1	Squad Portable Battery Charger	4
1.2	Other portable power generation applications	5
1.3	Other applications for Direct JP-8 generators	6
2	STTR A08-T007 Phase 1 Overview	7
3	Phase 1 Technical Objectives	8
3.1	Identification and evaluation of candidate liquid metal anodes	8
3.1.1	Requirements for direct hydrocarbon fuel cell anodes	8
3.1.2	Solid Metallic Anodes.....	8
3.1.3	Solid Non-Metallic Anodes- oxides	10
3.1.4	Liquid Anodes.....	11
3.1.5	Open Circuit Voltage	14
3.1.6	Preliminary Thermodynamic Data	15
3.1.7	Liquid Metal Anode Functionality	17
3.1.8	Fuel Flexibility	18
3.1.9	Efficiency.....	18
3.1.10	Tubular geometry	19
3.1.11	Previous work- Liquid Tin Anode SOFC	19
3.2	Characterization of relevant physiochemical processes and parameters 23	
3.3	Formulation of relevant mathematical models.....	25
3.3.1	Model Geometry	26
3.3.2	LTA-SOFC System with CO/H ₂ Fuel Mixture & CH ₄ /CO/H ₂ Fuel Mixture 33	
3.3.3	Effect of Parameters on LTA-SOFC Cell Performance	35
3.3.4	Transient Model for the LTA-SOFC Cell	39
3.4	Conceptualization of a 500 W liquid-metal anode fuel cell system	40
3.4.1	US Army Mission Needs	40
3.4.2	System Conceptual Design.....	42
3.4.3	System Level Flow Analysis	45

3.4.4	Conceptual Drawings/Diagrams.....	46
4	Summary of Phase 1 results.....	58
5	Recommended Next Steps.....	60
6	References.....	61

1 Mission need for small JP-8 generators

The US Department of Defense is the largest single consumer of oil in the world [1]. Under Directive 4140.25 the US military established a “one fuel forward” policy designating JP-8 as the single operating fuel for all military forward deployed equipment [2]. Liquid petroleum based logistic fuels have a significant volumetric and gravimetric energy density advantage compared to other fuels which makes them highly desirable for mobile/portable applications. In the field today nearly all military electrical power is generated by IC engine generators. Fuel cells are ideal for military field applications due to their high efficiency, quiet operation and operation on JP-8 allows the use of a readily available, high energy density fuel. However the complex hydrocarbon composition and high sulfur content makes operation on JP-8 difficult for conventional fuel cells. JP-8 reforming is difficult and a viable JP-8 reforming process has yet to be developed. A fuel flexible fuel cell capable of direct oxidation of common hydrocarbons such as JP-8 would significantly improve the battlefield power generation situation. The generally recognized merits of direct oxidation fuel cells include very high fuel efficiency of 55%-68% using hydrocarbons [4], system simplicity and cost.

1.1 Squad Portable Battery Charger

The proliferation of electronic devices on the battlefield has pushed US military portable power demand to an unprecedented level. This increase in portable power demand necessitates an increased need for portable power generators. A rechargeable power supply compatible with the JP-8 logistics fuel will enable the US military to:

- Simplify fuel supply chain management
- Support the military’s transition to rechargeable batteries, as a means to reduce the cost and logistic burden of supplying field power
- Reduce the amount of batteries needed to support squad missions

Plug-in battery chargers are currently available to support deployed forces and can be operated where there is a power infrastructure. However, a battery charger with an integrated generator that uses logistics fuel would provide independence from electric generators, vehicles, or the grid through stand-alone power generation in forward areas.

1.1.1.1 Army Power Division – CERDEC

The Army Power Division is the CERDEC agency, within the C2D Directorate, responsible to conduct research, development and engineering leading to the highest density, safest, most cost-effective, energy and environmental technologies to meet the Warfighter's portable and mobile application needs today and in the future. As such, the Army Power Division establishes objectives for candidate batteries and battery charging equipment for the US Army.

Army power applications serve a wide range of applications, including the following:

- Remote power for sensors, laptops in remotes areas, silent watch operations
- Portable power
- Robotic vehicle power
- Energy recovery
- Cogeneration

Power sources for these applications, as well as battery recharging units, should demonstrate the following qualities:

- Scalable
- Low Noise
- Solid-state
- Logistic-fuel adaptable

Army and Marine Corps studies have shown that the optimal power range to support battery charging for squad operations is between 50 and 500 Watts. The smallest capacity standard generator in the MEP inventory is 2 kW and is ill suited to support squad level battery charging. Fuel cells offer significant technological advantages for portable power applications due to the ease at which they can be scaled.

1.2 Other portable power generation applications

A direct JP-8 power generator can also meet other military mission needs. A power source below 1 kW could be used as a power source in a variety of applications, several of which include:

- Robotics to extend mission length by allowing extended sentry duty or long duration mobile operations. The successful use of small battery powered military robots, such as the Talon robot; to find and defeat roadside bombs has led to identification of new military applications. The development and deployment of more sophisticated longer-operating autonomous minesweeping robots could dramatically increase mine removal

productivity and prevent military and civilian casualties. Increased field power is needed for the advancement of these robots.

- Remote detectors (i.e. Boomerang shot detectors) or unattended sensor strings which require long duration operation and are difficult to refuel on a frequent basis.
- Silent watch operation; powering smaller discrete loads.

Today such missions typically utilize traditional batteries which limit mission duration. These field power applications are not easily addressed by existing IC engine gensets because of their size, noise, durability and high fuel consumption.

1.3 Other applications for Direct JP-8 generators

There are many generator options that exist in the 2 kW to 1 MW power range. However, development of a ruggedized quiet and efficient JP-8 fuel cell generator replacement for IC engine gensets would reduce generator fuel consumption and noise footprint. Additionally, new generator technology could be used to support emerging applications. For instance ONR recently has defined the need for a 10 kW under armor fuel cell APU based on JP-8. Thus, once Direct JP-8 fuel cell technology is introduced in applications such as squad battery charging, it is possible to envision scale up of the technology to ranges as high as 100 kW. Direct fuel cells offer the flexibility to accommodate the changing demands for field power.

2 STTR A08-T007 Phase 1 Overview

Recognizing the important gap that could be filled by a Direct JP-8 battery charger, the Army Research Lab initiated STTR A08 – T007. The tasks in Phase 1 of the STTR are shown below in Table 3.1.1-1 along with an overview of how each task will contribute to the development of a Direct JP-8 battery charger:

Number	Task	Importance to Direct JP-8 Battery Charger
1	<i>Identification and evaluation of candidate liquid metal anodes</i>	Identify and select the most promising fuel cell technology for Direct JP-8 application.
2	<i>Characterization of relevant physicochemical processes and parameters</i>	Provide technical characteristics of selected technology to guide design, development and modeling efforts
3	<i>Formulation of relevant mathematical models of the liquid-anode fuel cell</i>	Develop and utilize analytical tools which can assist engineering design and lab testing
4	<i>Conceptualization of a 500 W liquid-metal anode fuel cell system</i>	Determine how selected technology will be implemented in a battery charger system.

Table 3.1.1-1: STTR Phase 1 Tasks

3 Phase 1 Technical Objectives

3.1 Identification and evaluation of candidate liquid metal anodes

The purpose of this task is to identify potential liquid metal anode materials for a direct JP-8 fuel cell and select the most promising for further design and modeling work.

3.1.1 Requirements for direct hydrocarbon fuel cell anodes

A fuel-flexible fuel cell capable of direct oxidation of common hydrocarbons such as JP-8 is the ultimate technical challenge for fuel cell researchers. The development of liquid metal anodes for direct oxidation of hydrocarbons is a revolutionary advancement in the field. Potential candidates of liquid metal anodes include a group of liquid metals (Al, Ga, In, Sn, Sb, Tl, Pb, Bi and Po) and the adjacent transitional metals IB and IIB (Ag, Hg, Cd). Anodes and catalysts for the direct oxidation of hydrocarbon fuels must meet the following conditions:

- Reduce the activation energy for the oxidation of target hydrocarbons
- Provide a reaction zone where fuel molecules reacts with oxygen;
- Provide good transport of oxygen species in molecular, atomic or ionic form through its bulk or on surface, with good reduction/oxidation (redox) cycle tolerance
- Capable of transporting fuel species or their derivatives in situ through its bulk or on surface;
- Capable of capture and transporting charged species (ions or electrons);
- Capable of releasing reaction products;
- Compatible with fuel cell components, including the electrolyte and
- Acceptable cost, operating temperature, toxicity and availability.

3.1.2 Solid Metallic Anodes

Most common heterogeneous anode catalysts are solid either as a solid phase porous structure or as sparsely distributed solid phase particles on a high surface area support. The main advantage of a solid heterogeneous catalyst is that its reaction surface can be designed to be very large, increasing overall reaction rates. Noble metals and, to a lesser degree, solid oxides are well known as solid heterogeneous catalysts. Commonly used precious metal catalysts include Pt and bimetallic alloys such as Pt-Au, Pt-Ir, and Pt-Re. In general, solid heterogeneous metallic catalysts are almost exclusively a group of transition metals consisting of Pt, Pd, Ni, Ir, Rh, Co, Os, Ru, Ag and Cu, etc. The chemisorption and surface reactions of hydrocarbons on metallic surfaces have been

extensively studied. Davis and G. Somorjai summarized metallic catalysis of reforming of petroleum feed stocks, non-destructive skeletal dehydration, isomerization, and cracking.

For example, at intermediate temperatures above 600°C, Ni has sufficient catalytic activity to be used as a catalyst in reducing (anode) atmospheres. Thus Ni is used in MCFC. In SOFC Ni is also used, since a composite anode of Ni-YSZ can be used to support the electrolyte. Pt is an excellent catalyst and anode for all types of fuel cells however its use is limited because of high material cost.

Carbon formation is a roadblock for most solid metallic heterogeneous anode catalysts operating on complex hydrocarbons. From a scientific perspective Solid Oxide Fuel Cells using nickel anode catalysts are thermodynamically capable of direct oxidation of hydrocarbons and other carbonaceous fuels. However, real world engineering experience has shown that carbon and/or sulfur in these fuels create barriers to long term operation of conventional nickel based SOFC anodes. Carbon formation on the Ni anode causes a phenomenon known as anode puff-up or dusting; a complete disintegration of the Ni-anode under conditions favoring coke formation. Destruction of Ni anodes by hydrocarbons has been well documented [4, 5]. It had been also demonstrated that a mixture of CO₂ (20%) and CO (80%) will cause a complete destruction of the Ni/YSZ anode at 800°C in less than 16 hours. The current engineering solution to coking issues is to reform the fuel to a partial oxidized (POX) state. Such fuel reforming not only increases system complexity but also leads to substantial loss of fuel efficiency. In POX reforming processes fuel efficiency losses of more than 30% and up to 45%-50% can occur. Furthermore, there exist unresolved logistic issues for startup and shutdown of Ni anode/SOFC using reformat. Unless there is a hydrogen source or other non-coking gas available on site to blanket the fuel cell stack during startup and shutdown, coking conditions are essentially unavoidable. There is currently no solid metallic anode with good catalytic activity that avoids dusting under coking conditions, which eventually will lead to anode destruction.

Sulfur is the other known road block for solid metallic anodes. Military logistics fuels and coal contain substantial amount of sulfur. JP-8, JP-5 and NATO 76 fuels have maximum sulfur levels of 3,000ppm, 3,000ppm and 10,000 ppm respectively [6,7]. In these fuels sulfur is chemically bonded with the carbon backbone. Selective sulfur removal from these fuels has proven rather difficult and a whole field of science and technology has been devoted to this endeavor. Prior to CellTech Power's LTA-SOFC, no fuel cell technology has demonstrated use of high sulfur fuel without removing or reducing the sulfur level. Metallic catalysts, i.e. Ni or Pt, are rapidly poisoned by sulfur. The dominating thermodynamic reaction is the formation of metal sulfides or sulfates, not the desired electrochemical reduction reaction. The sulfur species which are formed

deactivate the catalysts and in the case of Ni destroy the solid catalyst microstructure and anodic lattice by via the liquid phase NiS.

3.1.3 Solid Non-Metallic Anodes- oxides

Solid heterogeneous oxide catalysts do not use expensive Noble metals and have shown improved tolerance to coking. These solid oxides offer compelling alternatives for direct oxidation of hydrocarbons. These catalysts are exclusively a group of oxides made of multi-valence metals, V(2,3,4,5), Ce (3,4), Nb (3,5), Mo (2,3,4,5,6) and W (2,3,4,5,6), etc. Combined with good electrical current conductors, some of these oxides are suitable anode candidates (i.e. CeO_2/Cu).

First, vanadium oxides have been demonstrated as a good catalyst for direct oxidation of carbonaceous matter, including carbon and hydrocarbons. V_2O_5 has been used extensively for the oxidation of sulfur to make sulfuric acid. Vanadium carbide used as a fuel cell anode has been evaluated by Japanese researchers and CellTech Power. Its favorable catalytic activity initially raised expectation of low temperature direct oxidation of hydrocarbons in a fuel cell. However, extensive data obtained from both theoretical modeling and experimental results confirmed that vanadium oxides are not suitable for use as an SOFC anode due to the destruction fuel cell components such as the doped zirconium oxide electrolyte.

Next, $\text{Gd}_2\text{Ti}_{1.4}\text{Mo}_{0.6}\text{O}_7$ has been proposed as a sulfur tolerant anodic catalyst. Similar to vanadium oxides, Mo is a multi-valence element with +3, +4, +5 and +6. However, Mo containing solid oxides are not suitable for redox cycle since the phase is inherently unstable. Furthermore, Mo oxides are known to cause destabilization of doped zirconia electrolyte in a matter of hours or days. V, Mo, Nb and W oxides have shown the same detrimental impact on doped zirconia electrolytes. However, it is possible that these highly reactive oxide catalysts could be used as an anode if a compatible electrolyte and the rest of fuel cell balance of plant could be developed. Pursuit of these oxide anodes with an unknown electrolyte and unproven balance of plant is outside of the scope of this program.

Additionally, alkaline rare earth oxides like Ce are viable oxidation catalysts with wide applications such as reduction of CO, NO and hydrocarbon emissions in automobile catalytic converters. Ce oxides with +3 and +4 valences (and transitional states between 3 and 4) possess suitable oxygen-storage capacity to promote oxidation of hydrocarbons and CO. Like all rare alkaline earth metals and alkaline earth metal oxides, Ce oxides are strong bases. They react preferentially with acidic sulfur and its compounds, S, SO_2 and H_2S . These reactions of cerium oxides with sulfur and its compounds lead to poisoning and have been reasonably well studied. For example ceria (Ce oxides) has been used as an absorber for removing H_2S and SO_2 . In SOFCs the Cu/CeO_2 anode has been shown to lose its activity at 400-500 ppm sulfur, partially due

to formation of more stable Ce sulfate $\text{Ce}_3(\text{SO}_4)_2$, leading to loss of catalytic activity and destruction of the anodic lattice.

The most publicized direct oxidation fuel cell is the Cu/CeO₂ anode/SOFC introduced in the early 2000's. Indeed button cells operating at about 800°C have shown substantial improvement over Ni anodes in direct conversion of hydrocarbons. However, Cu and eventually all solid ferrous and non-ferrous metals have shown some tendency to disintegrate into finer powder (dusting or puffing) when exposed to coking gases. The disintegration rate of Cu is slower than Ni, but eventually leads to the collapse of the Cu anode. Accumulation of non-reactive graphitic carbon is also a problem. Direct introduction of hydrocarbons into cells at 800°C leads to spontaneous pyrolysis, forming many types of carbon, including soot, amorphous and graphitic. The reactive portion such as nano scale particles have sufficient reaction rate at 800°C and are consumed, leaving an accumulation of less reactive or non-reactive forms including graphitic carbon. This carbon build up, especially adjacent to the fuel inlet leads to eventual failure of the stack. At temperatures around 1,000°C all forms of carbon are chemically reactive but this operating temperature is not feasible to use Cu (morphological changes and coking). Fuel reforming or processing is still apparently a necessity for Cu/CeO₂ to avoid coking at the fuel inlet, particularly with the more complex fuel passageways used in planar SOFC's.

Other recent studies of possible sulfur tolerant anode materials for SOFCs include doped LaSr oxides for use in hydrogen containing 1% H₂S possibly up to 10%. La and Sr oxides are strong bases. Similar to Ce oxides, thermodynamic data reveals the doped LaSr oxides react with acidic sulfur and its compounds to form stable sulfate, sulfite or sulfide leading to eventual collapse of the anodic lattice.

Destabilization of solid anodic catalysts by coking and sulfur remains a formidable technical challenge. So far there were no known solid heterogeneous catalyst (either metallic or oxides,) that has proven suitable as an anode for high sulfur content hydrocarbon fuels such as JP-8.

3.1.4 Liquid Anodes

Liquid heterogeneous catalysts provide an interesting alternative as an anode for fuel cells using JP-8. A liquid anode, being in a fluid state, can be designed as a non structural component of the fuel cell system. This type of design makes it possible to isolate structural changes in the anode (from temperature or chemical changes) from the rest of the fuel cell, avoiding the destruction of the whole fuel cell and provides the ability to replace the anode. However liquid heterogeneous catalysis has been much less studied compared to solid heterogeneous catalysis or homogeneous catalysis.

The concept of a liquid anode fuel cell for direct oxidation of fuel is not entirely new. Liquid alkaline hydroxides of Na, K and Li have been used for direct oxidation of carbon, and perhaps for hydrocarbons. W.W. Jacques in the late 19th century demonstrated a kW-scale carbon battery. In his device carbon rods were oxidized to CO₂ to produce electricity. Unfortunately the CO₂ further reacted with alkaline hydroxides to form carbonates causing depletion of the alkaline hydroxides. SARA Inc worked on this type of fuel cell up to 2006 when they finally documented the irreversible carbonate formation and abandoned their effort.

A concept of fuel cell capable of direct oxidation of common fuels (hydrocarbons), using molten salts or molten carbonates was studied for over 30 years by the Swiss chemist E Baur during early 20th century. His efforts and others later evolved into the birth of the molten carbonate fuel cell, a molten electrolyte made of carbonates of alkaline metals such as Li, Na and K. Molten carbonate/salt catalysis for direct conversion/oxidation of light hydrocarbons like methane has been well studied. Commercial units are available (for example Fuel Cell Energy's Molten Carbonate Fuel Cell called a "direct fuel" fuel cell) and the latest SRI approach of mixed molten carbonates of alkaline metals as a liquid anode. A molten carbonate/salt anode using high sulfur fuel such as JP-8 (3,000 ppm) will have limitations since sulfur will form more thermodynamically stable sulfate or sulfite leading to irreversible consumption of the anode. Molten carbonate/salt technology is currently under developed by several commercial entities.

Up to 2006 there was no known direct oxidation fuel cell using JP-8. At that time CellTech Power demonstrated that the Liquid Tin Anode SOFC is capable of direct oxidation of hydrocarbons such as JP-8 without any fuel reforming or processing or sulfur removal.

3.1.4.1P-orbital-electron metals as liquid heterogeneous anodic catalysts

Metals containing unsaturated or unpaired p-orbital electrons have unique physical, chemical and electrochemical properties. Initial criteria for their suitability as an anodic catalyst include melting point, ΔG of the oxidation reaction and hydrocarbon reactions and Open Circuit Voltage, all which have been calculated using thermodynamic data. This group of metals (Al, Ga, In, Sn, Sb, Tl, Pb, Bi and Po) and the adjacent transitional metals IB and IIB (Ag, Hg, Cd) have low melting points, well below 1,000° C. All hydrocarbons chemically consist of hydrogen and carbon. The activation energy needed for a carbon reaction is greater than that for a hydrogen reaction. The metal oxide reductions with carbon at 1,000°C are listed in Table 3.1.4-1.

Reduction	ΔG (kcal/mole)
$1/1.5\text{Al}_2\text{O}_3 + \text{C} = \text{CO}_{2(\text{g})} + 2/1.5\text{Al}$	107.7
$1/1.5\text{Ga}_2\text{O}_3 + \text{C} = \text{CO}_{2(\text{g})} + 2/1.5\text{Ga}$	12.6
$1/1.5\text{In}_2\text{O}_3 + \text{C} = \text{CO}_{2(\text{g})} + 2/1.5\text{In}$	-12.3
$\text{GeO}_2 + \text{C} = \text{CO}_{2(\text{g})} + \text{Ge}$	-14.5
$\text{SnO}_2 + \text{C} = \text{CO}_{2(\text{g})} + \text{Sn}$	-20.3
$1/1.5\text{Sb}_2\text{O}_3 + \text{C} = \text{CO}_{2(\text{g})} + 2/1.5\text{Sb}$	-33.6
$1/1.5\text{Bi}_2\text{O}_3 + \text{C} = \text{CO}_{2(\text{g})} + 2/1.5\text{Bi}$	-58.2
$1/1.5\text{Tl}_2\text{O}_3 + \text{C} = \text{CO}_{2(\text{g})} + 2/1.5\text{Tl}$	-87.1
$\text{PbO}_2 + \text{C} = \text{CO}_{2(\text{g})} + \text{Pb}$	-88.3
$\text{PoO}_2 + \text{C} = \text{CO}_{2(\text{g})} + \text{Po}$	-93.3
$2\text{HgO} + \text{C} = \text{CO}_{2(\text{g})} + 2\text{Hg}$	-113.7
$2\text{Ag}_2\text{O} + \text{C} = \text{CO}_{2(\text{g})} + 4\text{Ag}$	-116.8

Table 3.1.4-1 Reduction of p-orbital electron metal oxides by carbon at 1000°C

Both Al and Ga oxide reduction reactions by carbon have positive ΔG , indicating that their oxides are more stable and would not be reduced back to metals by carbon at a temperature of 1,000°C since the reaction is not spontaneous. Therefore Al and Ga would make poor catalysts. The rest of the metal oxides have negative ΔG , indicating their reduction is spontaneous. These p-orbital electron metals (except for Al and Ga) show reversibility of redox reactions, thus they are capable of catalyzing direct oxidation of hydrocarbons. P-orbital metal oxides (except for Al and Ga) can oxidize hydrocarbons at temperatures below 1,000°C, a temperature where SOFC operates. Their reversibility of redox reactions makes these liquid metals a potential candidate as a liquid heterogeneous catalytic anode.

3.1.4.2 Oxidation Reaction

Thermodynamic data (Gibbs Energy, ΔG) for the oxidation of P-orbital-electron metals with oxygen at 1,000°C and their melting points are listed in Table 3.1.4-2.

**Table 3.1.4-2 Oxidation reaction and melting points
of P-orbital electron metals**

Oxidation	ΔG (kcal/mole)	Melting Point (°C)
$4/3\text{Al} + \text{O}_{2(g)} = 2/3\text{Al}_2\text{O}_3$	-202	660
$4/3\text{Ga} + \text{O}_{2(g)} = 2/3\text{Ga}_2\text{O}_3$	-107	29.7
$\text{Ge} + \text{O}_{2(g)} = \text{GeO}_2$	-80.1	938
$4/3\text{In} + \text{O}_{2(g)} = 2/3\text{In}_2\text{O}_3$	-77.3	156.6
$\text{Sn} + \text{O}_{2(g)} = \text{SnO}_2$	-74.3	232
$2\text{Cd} + \text{O}_{2(g)} = 2\text{CdO}$	-61.6	321
$4/3\text{Sb} + \text{O}_{2(g)} = 2/3\text{Sb}_2\text{O}_3$	-60.9	630
$2\text{Pb} + \text{O}_{2(g)} = 2\text{PbO}$	-45.5	327
$4\text{Tl} + \text{O}_{2(g)} = 2\text{Tl}_2\text{O}$	-36.4	304
$4/3\text{Bi} + \text{O}_{2(g)} = 2/3\text{Bi}_2\text{O}_3$	-36.4	271
$\text{Po} + \text{O}_{2(g)} = \text{PoO}_2$	-1.3	254
$2\text{Hg} + \text{O}_{2(g)} = 2\text{HgO}$	19.1	-39
$4\text{Ag} + \text{O}_{2(g)} = 2\text{Ag}_2\text{O}$	22.2	962

All p-orbital electron metal oxidation reactions are spontaneous and exothermic (except for transitional metals Hg and Ag). The ΔG of Oxidation Al and Ga is more negative, -202 and -107 kcal/mole respectively, indicating their binding energy with oxygen is very strong and they will not readily give up oxygen as required for a catalyst for oxidation of hydrocarbons. The rest of these metals have a moderate to low negative, some even positive ΔG , indicating their readiness to give up oxygen, reversibility of Redox, and under normal fuel cell operational conditions their potential suitability as a catalyst for oxidation of hydrocarbons. The ΔG threshold as a catalytic anode for SOFC is estimated to be about -80 kcal/mole. More negative values imply oxygen bonding is too strong and thus the material is not a good catalyst.

3.1.5 Open Circuit Voltage

Open Circuit Voltages (OCV) of Bi, Sb, Sn and In oxidation with oxygen, in relationship with C, CO and Hydrogen (derivatives of any hydrocarbon) at various temperatures are shown in Figure 1. OCV is an equivalent in electrochemistry to the term of ΔG . There exists temperature thresholds where direct oxidation of fuel (H_2 , C, CO and

hydrocarbons) by these oxides occur, at about 750°C, 650°C, 410°C and 160°C for In, Sn, Sb and Bi respectively.

In general the OCV of a metal oxidation decreases as the temperature increases. For instance, $2\text{In} + 3/2 \text{O}_2 = \text{In}_2\text{O}_3$, at ambient temperature has an OCV of 1.45 V reducing to 0.85 V at 1,000°C degree. However carbon is an exception: for $\text{C} + \text{O}_2 = \text{CO}_2$, it's Gibbs Energy (ΔG) and its OCV (1.02 V) have little to do with temperature as shown by the flat line in Figure 1; for $2\text{C} + \text{O}_2 = 2\text{CO}$, the OCV actually increases as temperature increases. This implies that thermodynamically any metal oxide can be reduced back to metal by carbon at a proper temperature (a threshold). Hydrogen oxidation is similar to a metal, but its OCV is less sensitive to temperature as shown by the less steep slope in Figure 1. Similar to carbon there are temperature thresholds for hydrogen also. These temperatures for Bi, Sb, Sn and In are <0°C, < 0°C, 600°C and 900°C respectively.

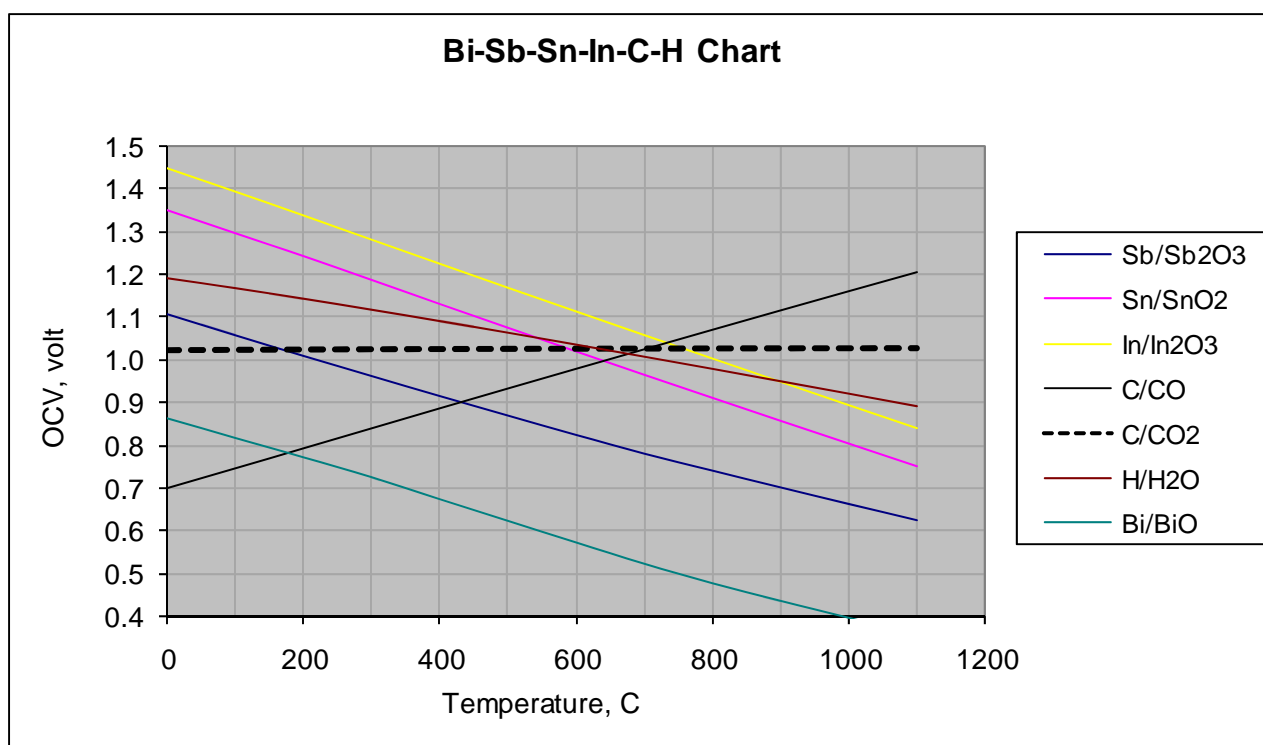


Figure 1 OCV of oxidation reactions of Bi, Sb, Sn and In as well as C, CO and H₂.

P-orbital electron metals as liquid heterogeneous catalysts for direct oxidation of hydrocarbons, their ranking of Redox activities, and their projected temperature of operation for use as a fuel cell anode are listed in Table 3 below.

3.1.6 Preliminary Thermodynamic Data

The group of molten metals (Ge), In, Sn, Cd, Sb, Pb, Po, Tl, Bi, Hg and Ag would be suitable as a liquid heterogeneous anodic catalyst for direct oxidation of hydrocarbons.

This group of metals can be further divided into three sub groups according to their projected redox ability at different temperatures: (1) Group II, the high temperature group (more negative ΔG , or higher OCV) of (Ge), In and Sn would be suitable for high temperature fuel cell operation at 700°C or higher (up to 1,000°C); (2) Group III the intermediate temperature group (lesser negative ΔG) of Cd, Sb and Pb would be suitable for intermediate temperature fuel cell operation at 400°C or higher; and (3) Group IV the low temperature group (low or positive Delta G) of Po, Tl, Bi, Hg and Ag would be suitable for low temperature fuel cell operation at ambient temperature and up. Of course at lower temperatures some of these metals are not in liquid state, they would have to be used at elevated temperature or in an alloy. Many of them are volatile and their use at elevated temperature is limited. These conclusions are based on thermodynamic analysis. Fuel oxidation rates are governed by their kinetics also. So far no kinetic modeling or analysis has been performed on these liquid metals. At any given temperature, the catalytic activity of the group (Ge), In, Sn, Cd, Sb, Pb, Po, Tl, Bi, Hg and Ag is projected to be at ascending order. That means, Sn would be a relatively mediocre catalyst, just slightly more active than In, Sb would be more active than Sn, and Bi would be even more active, etc.

**Table 3.1.6-1 Ranking of p-orbital metals
as
catalysts for direct oxidation**

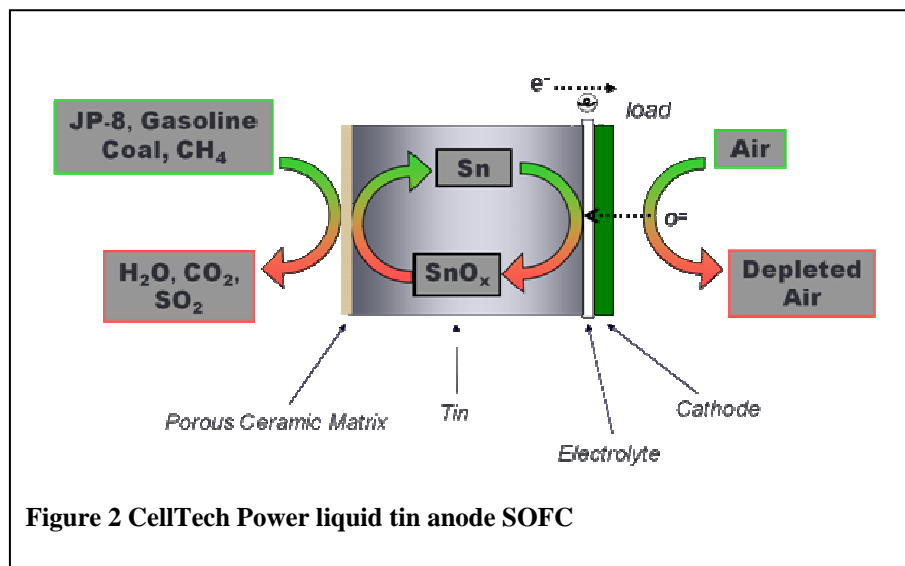
p-orbital electron metal	Redox activity	Temperature of operation °C
Al	Group I	> 1,000
Ga	Group I	> 1,000
Ge	Group II	> 700
In	Group II	> 700
Sn	Group II	> 700
Cd	Group III	> 400
Sb	Group III	> 400
Pb	Group III	> 400
Tl	Group IV	> 20
Bi	Group IV	> 20
Po	Group IV	> 20
Hg	Group IV	> 20

Ag	Group IV	> 20
----	----------	------

The electrochemistry and heterogeneous catalysis of liquid tin anode SOFC for direct oxidation of hydrocarbons, and its tolerance of coking and sulfur have been studied at CellTech Power. As discussed in Section 3.1.11, CellTech [3] has considerable experience with cells, stacks and systems using liquid tin. Therefore, for this STTR, CellTech Power proposes to use a tin anode for the direct JP-8 battery charger.

3.1.7 Liquid Metal Anode Functionality

In contrast to a solid state fuel cell anode, the liquid metal anode acts as an intermediary between the fuel and the oxygen ions. This is shown schematically in Figure 2 and Figure 3. The oxides or the oxygen solubility in the liquid metal allows the



electrochemical reaction at the electrolyte anode interface to proceed without a phase change of the anode metal itself. The initial anode reaction is electrochemical ($M + xO^{2-} \rightarrow MO_x + 2xe^-$); subsequent anode reactions are purely chemical. Oxygen or oxides dissolved in the molten metal then diffuse through the metal bulk to the fuel where it reduces the metal oxide back to metal and oxidizes the fuel source. If fuel molecules are soluble, they may be dissolved in the molten metal anode and react with oxygen diffused from the electrolyte. This fuel source can be hydrogen (H_2), CO or hydrocarbons, but due to the unique characteristics of the liquid metal anode described above, it can also be solid carbon or liquid hydrocarbons. In fact the heterogeneous liquid metal anodic catalyst actually participates in intermediate reaction steps, possessing characteristics of both solid heterogeneous catalysis (interface) and homogeneous catalysis (bulk diffusion). In the case of solid carbon, the

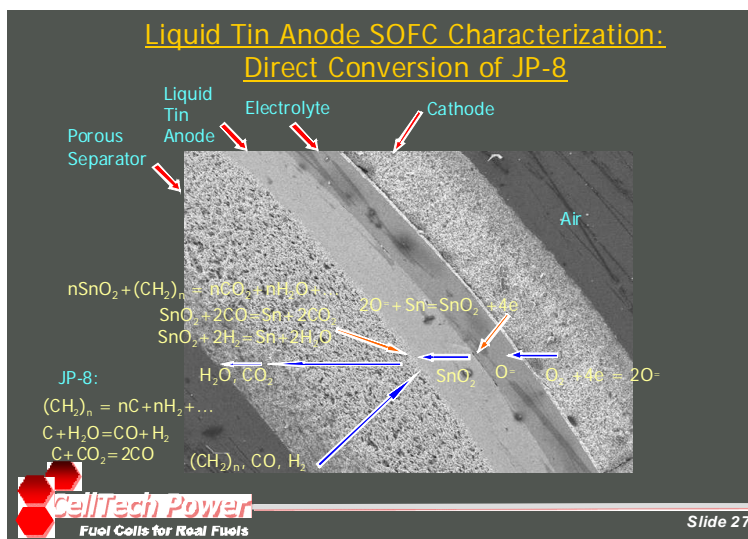


Figure 3 Direct JP-8 oxidation in a liquid tin anode SOFC

final anode exhaust products will be CO and carbon dioxide (CO₂); if logistics fuels are used, exhaust products will include H₂S, SO₂ in addition to CO, CO₂, and H₂O.

3.1.8 Fuel Flexibility

While the focus of this project is on a direct JP-8 power source, fuel flexibility can provide additional operational flexibility for military users, allowing the option to use of opportunity fuels or renewable fuels for example. In addition, a technology with fuel flexibility will likely have a broader range of commercial markets, increasing production volume and potentially lowering the cost of JP-8 generators. A properly designed tubular, external anode design for liquid anode fuel cells will allow solid, liquid or gaseous fuels to be introduced directly into the fuel cell. Using this architecture, CellTech has tested the liquid tin anode SOFC on natural gas, diesel, biomass, carbon and coal as well as JP-8.

3.1.9 Efficiency

We expect the direct oxidation fuel cell to be the most efficient system of any known generation technology. The consulting firm of TIAX, LLC of Cambridge, MA has analyzed fuel efficiency for a direct oxidation SOFC at 5 kW, and their findings compared with traditional SOFC (Ni anode) using diesel as fuel are listed below:

Table 3.1.9-1 -Efficiencies of Direct oxidation SOFC and traditional SOFC (Ni)

	Traditional SOFC	Traditional SOFC	Direct Oxidation	Direct Oxidation
Fuel Utilization	90%	70%	90%	70%
Stack Efficiency (LHV)	47%	36%	61%	47%

Cathode Excess Air	806%	779%	444%	400%
Parasitic Loads, % (W)	14.5% (847)	14.4% (838)	8.1% (442)	7.6% (411)
System Electric Efficiency (LHV)	35%	29%	56%	44%

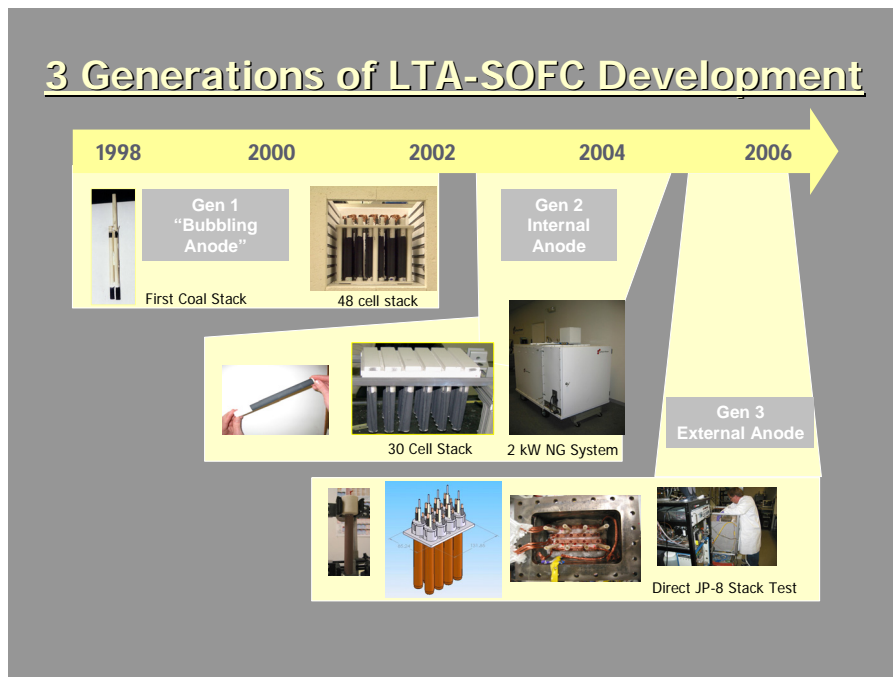
According to TIAX a direct oxidation SOFC would have stack (cell) efficiency of 61% and system at 56%, while traditional SOFC (Ni anode) 47% and 35% respectively. CellTech Power's estimation of direct oxidation fuel cell using carbon as a fuel would give stack (cell) efficiency at 65-68% and system 58-62%. CellTech Power has measured fuel efficiency in a single cell using JP-8 and carbon to be 43% and 60% respectively. Further improvement in fuel efficiency above these experimental values is expected by (1) increased fuel utilization, (2) reduced parasitic leakage on the test stand and (3) reduced cell internal resistance and polarizations

3.1.10 Tubular geometry

Planar solid oxide fuel cell is sometimes assumed to have higher specific power compared to Westinghouse-Siemens type tubular fuel cells. But planar SOFC for direct oxidation of hydrocarbons such as JP-8 is not a viable architecture: it only works at single cell level. For a multi-cell stack an intricate fuel manifold is required for balanced fuel delivery to each hot cell, creating formidable coke formation challenges. Franklin Fuel Cell Inc. (now defunct) developed single planar SOFC discs with a CeO₂/Cu anode, however they did not succeed in demonstration of direct oxidation of hydrocarbons such as diesel or JP-8 at the multi-cell stack level. CellTech Power's unique exterior anode tubular architecture was developed to allow difficult, coke forming fuels like JP-8 to be injected into a common anode chamber without coke formation. Our stacks share a common fuel injection point. CellTech Power strongly believes that any development effort proposing planar SOFC for direct oxidation of hydrocarbons is will not be successful at the stack and system level.

3.1.11 Previous work- Liquid Tin Anode SOFC

The Liquid Tin Anode fuel cell has been under development by CellTech since our first mini-stack was operated in 1998. Figure 4 shows the 3 generations of LTA-SOFC Cells



that have been developed.

CellTech has fabricated over 10,000 single cells and learned how to combine them physically and electrically into stacks while assuring good thermal and chemical environments. CellTech has built integrated, autonomous LTA-SOFC systems and in 2004 we operated our full scale- 2 kW prototype on natural gas for over 2000 hrs, using the Generation 2 design. Experimental results have been obtained using the liquid tin anode fuel cell for a wide variety of fuels. Table 3.1.11-1 shows the fuel flexibility and high experimental efficiencies that have been obtained by CellTech using LTA-SOFC.

Figure 4 CellTech has developed 3 generations of Liquid Tin Anode SOFC's

Fuel	(mV)		Total test time (cells x hrs)
	Cell, max	Stack	
Hydrogen	50	30	2,000,000
Natural Gas		29	100,000
JP-8/Diesel	43	N/A	3,000
Plastic	43-49	26	1,000
Biomass&char	34-60	N/A	100

Table 3.1.11-1 - The Liquid Tin Anode SOFC has demonstrated broad fuel flexibility and high efficiency

Table 3.1.11-2 provides a history of the progressive improvement of the LTA-SOFC toward the goal of a reliable, efficient direct conversion device for hydrocarbon fuels.

Table 3.1.11-2 Liquid Tin Anode Design History

	Year	Max Power (mW/cm ²)		Anode Configuration Cell size (Ø X L cm)	Key Findings/Accomplishments
		JP-8	H ₂		
Gen 1 (Private funding)	2000	N/A	20	Internal pool of tin 1.0 x 15	Validated tin anode concept for direct oxidation of fuels in single cells. Gas bubbles through tin, interfering with power output, fuel delivery and causing cell failures
Gen 2 (Private funding)	2002 to 2005	20	40	Internal with ceramic separator 1.5 x 10	Invented anode current collectors Invented cathode current collectors w/o hot zone interconnect Introduced porous ceramic separator between gaseous fuels and tin. Made of special material MIECs (Mixed Ionic and Electronic Conductor) Demonstrated stand alone kWatt system for hydrogen and NG (2000 hrs). Required non-sooting gaseous fuel distributed into each cell.
Gen 3 (DARPA MISER Ph 1)	2005	40	80	External with ceramic separator 1.5 x 15	Introduced external separator for direct oxidation of logistics and solid fuels in single cells and stack. Proof of concept: direct oxidation of logistic fuels fuel cell system, scalable to 5 kW. JP-8 with sulfur 1,341 ppm: 200 hrs and fuel efficiency up to 40%. Need to reduce cell electric resistance especially cathode circumferential loss. Need to reduce anode polarization especially diffusion losses in separator and tin
Gen 3.1 (DARPA/ Army)	2007	100	200	External w high porosity ceramic separator and thin tin layer 1.0 x 10	Achieve porosity of separator 60-70%, with common ceramics of YSZ, Al₂O₃ and mullite. Achieve tin thickness of 300-500 micron. Reduce cell electric resistance to less than 30 m-ohm with a new Daisy shaped cathode in a smaller cell. Complete development of fabrication techniques for separator, electrolyte tube, cathode tube, and assembly. Further improvement of cell performance may be difficult: requiring precisely dimensional match of separator and electrolyte and/or work on JP-8 fuel

					characteristics
Gen 3.2 (ONR)	2008 to 2010	160		External w high performance current collectors and improved cell packing density. 1.0 x 10	High performance current collectors allow more compact external form factor.

3.1.11.1 LTA-SOFC Gen 3.0

With DARPA support CellTech has developed a third generation cell specifically for the direct fuel conversion of solid and liquid fuels including logistics fuels. As shown in Figure 5, the Gen 3 cell is tubular, the most mature and durable SOFC configuration.



Figure 5 - Gen 3.1 operates directly on JP-8 and is ready for integration into a battery charger.

The Generation 3.0 cell designed in 2005 for the DARPA MISER program demonstrated the feasibility of direct JP-8 power generation and produced about 3 watts per cell and operated

		Achievement
		3.3 Watts
Power Density	100 mW/cm2	120 mW/cm2
Fuel Efficiency	28% @ 40 mW/cm2	40% @ 75 mW/cm2
Life	100 hours	110 hours
Thermal Cycling	10 cycles	13 cycles

on JP-8 as well as plastics. A single cell was operated for 200 hours on JP-8, demonstrating the possibility that the LTA-SOFC for military power generation.

The Gen 3.1 cell was designed for a battery charger and other sub-kilowatt portable power missions. The Gen 3.1 has demonstrated a power output of over 3 watts per cell but is 4 times smaller and lighter than the Gen 3.0. Individual cells interlock to form a stack without complex manifolds or support structure. To maximize system availability, individual cells can be replaced, a feat which is impossible in PEM or conventional planar Solid Oxide fuel cell stacks.

3.1.11.2 LTA-SOFC Gen 3.1

CellTech has developed and tested the Gen 3.1 cell under Army contract W911NF-07-C-0032 sponsored by Army CERDEC and DARPA DSO. The program started in January 2007 and ended in January 2008. Cell performance targets for this program were derived from requirements for a 250 watt direct JP-8 battery charger. Cell performance goals and achievements for this program are shown in Table 3.1.11-3. The Gen 3.1 design met or exceeded all cell-level and stack level program performance goals (power density, efficiency, durability, thermal cycling).

3.2 *Characterization of relevant physiochemical processes and parameters*

The purpose of this task is to define the governing processes and equations for the selected liquid metal anode fuel cell technology.

The liquid tin anode has a unique battery function which comes from a direct oxidation of metallic tin. Sn oxidation is shown in Eq (1), at 1000°C degree,



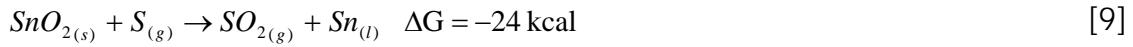
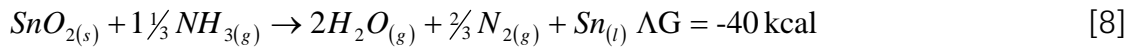
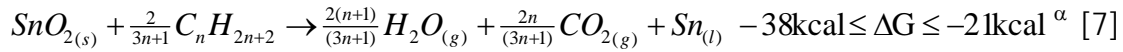
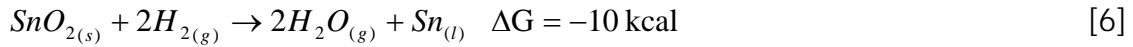
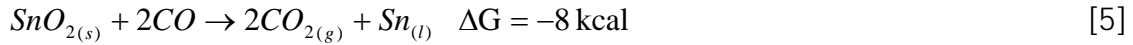
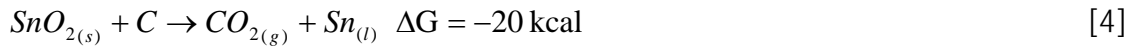
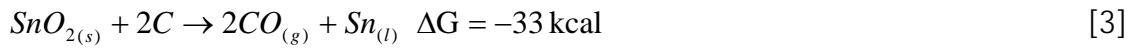
where the Gibbs Energy of -74kcal/mol gives an equivalent of an OCV of 0.78 volts, and (l) and (s) stand for a liquid and a solid state respectively.

The liquid tin anode fuel cell/battery can also be electrically recharged. Electrically recharging is a reduction reaction by reversing direction of an electrical current. Oxygen ions in anode are driven out by an applied electric field through electrolyte, releasing at cathode. This is identical to an electrically rechargeable battery such as Ni/Cd. Taking Sn as an example, the recharging reaction is



where (a) stands for tin oxide activity in a liquid tin anode. It is interesting that a liquid anode cell can be charged to an OCV higher than equilibrium (0.8 V) as shown in Eq (1). This is because its oxide activity can be less than one when unsaturated.

The liquid tin anode's ability to be charged by carbonaceous fuel is shown in Fig 3 and subsequent equations of (3) to (7). Chemically (fuel) recharging is a reduction reaction, using fuel to reduce metal tin oxides to metal tin. In fact fuel not only includes all carbonaceous such as charcoal, wood, paper, plastics and hydrogen, but also those containing nitrogen and sulfur as shown in equations of (8) and (9). Simplified fuel reduction reactions are, at 1000°C degree:



^α Range of ΔG values are based on saturated hydrocarbons CH₄ to C₃₂H₆₆, JP-8 can be approximated as Cetane C₁₆H₃₄ with ΔG = - 158 kJ

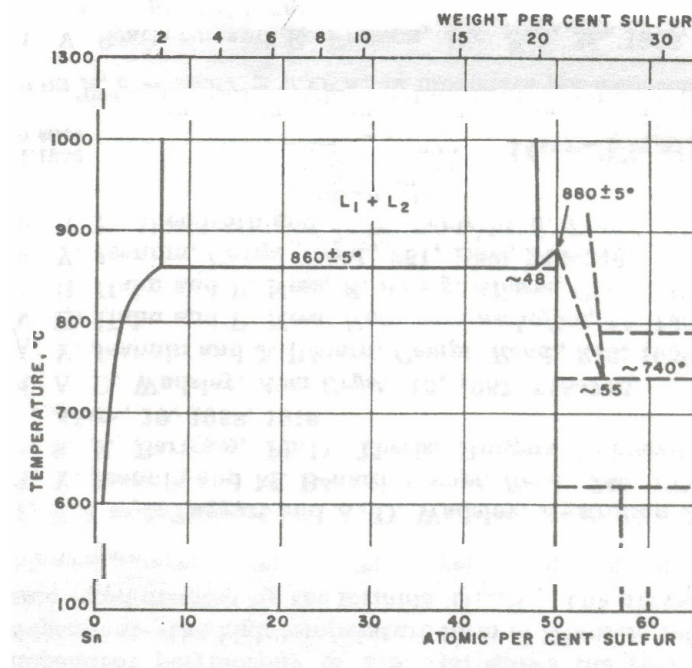


Figure 6 Sn-S phase diagram

These fuel reductions, Eqs (3) to (9), are thermodynamically favorable and spontaneous as evidenced by their negative Gibbs Energy. Eq. (7) using hydrocarbons as fuel is more complicated than the simplified equation itself because of thermal decomposition when exposed to a hot liquid anode. JP-8 is a complex mix of hydrocarbons and breaks down to smaller species such as hydrogen, carbon and methane, etc at elevated temperatures.

CellTech has demonstrated that using tin as an anode catalyst; sulfur is a fuel not a poison. As shown in Eq (9), sulfur is oxidized to SO_2 (or H_2S depending on fuel cell operational conditions). Figure 6 is a phase diagram of S-Sn. At or above 840°C , all Sn and sulfur compounds are in liquid state. The high solubility of sulfur in molten tin (8at% at 1000°C) allows dissolved sulfur and tin sulfides to be oxidized partially to SO_2 and carried out with anode exhaust. Steady performance has been demonstrated using JP-8 containing 1,350 ppm sulfur for 200 hours without any fuel process or reforming. In a separate test, a mix of H_2 , CO and CO_2 spiked with 200 ppm H_2S ran for 2 weeks continuously without any noticeable degradation in performance. In yet another test, up to 7% of sulfur in form of tin sulfite was introduced into the tin anode and the cell showed no sign of degradation.

3.3 Formulation of relevant mathematical models

Summary

A detailed electrochemical model (steady state and transient) [9] to simulate the performance of the Liquid Tin Anode (LTA)-Solid Oxide Fuel Cell (SOFC) system was developed using Comsol Multiphysics numerical simulation package. The Phase I work period consisted of three main developments in the modeling part and are mentioned below:

a) A steady state electrochemical model was developed for the LTA-SOFC system to simulate electrochemical performance for various inlet fuels (H_2 , CO , & CH_4).

b) A framework for developing a LTA-SOFC model system utilizing JP-8 as a fuel was also developed by integrating the Comsol Multiphysics model with the Reaction Engineering Lab module (REL). The modeling layout of REL has the capability to incorporate mathematical equations corresponding to multiple simultaneous chemical reactions, their reaction mechanisms and corresponding reaction kinetics. This feature will extremely simplify the procedure for simulating complex fuel species such as JP-8, where more than 100 known chemical reactions have to be accounted for to accurately describe the kinetics of JP-8.

c) A transient one-dimensional model was also developed for the LTA-SOFC system using Comsol Multiphysics.

3.3.1 Model Geometry

This section summarizes the work done by USC in developing electrochemical models for the LTA- in collaboration with CellTech. Initially, a 1-D radial axisymmetric model was developed to simulate the performance of a tubular LTA-SOFC (Cell Tech design) using H_2 as anode inlet fuel and air as cathode inlet fuel.

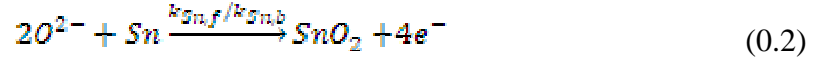
There are multiple physical domains within a single LTA-SOFC cell. The system that was considered for model development in Phase I of this project corresponds to the cylindrical design cell developed by Cell Tech as shown in Figure 7. The corresponding modeling domain (in the r-coordinate) is also shown in Figure 7. Air flows down a central channel ($0 < r < R_0$) in the reactor and continues to diffuse into the porous cathode ($R_0 < r < R_1$). At the end of the porous cathode (R_1), oxygen is reduced through four electron transfer to produce oxide ions (O^{2-}). The oxide ions then migrate through the ceramic electrolyte ($R_1 < r < R_2$) which is made from Yttria-Stabilized Zirconia (YSZ), and an O^{2-} ion conductor. On the anode side of the electrolyte (R_2), the molten tin is oxidized by the O^{2-} , producing SnO_2 and releasing four electrons. The electrons pass through the external circuit to the cathode and are available for the reduction of O_2 at the cathode. The tin oxide (SnO_2) diffuses through the LTA in the region $R_2 < r < R_3$ and it reacts chemically at R_3 to oxidize the fuel at the tin-separator interface and SnO_2 is reduced regenerating elemental Sn. Meanwhile, fuel diffuses (and potentially decomposes and/or reacts with product water) from the outer fuel chamber (R_4)

through the porous separator ($R_3 < r < R_4$) to the tin-separator interface. The overall reaction scheme considering O_2 and H_2 as the cathode and anode fuel is written as

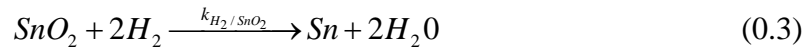
Electrochemical Reduction reaction at the cathode/YSZ interface: (R₁)



Electrochemical Oxidation reaction at the LTA/YSZ interface: (R₂)



Chemical Reduction of SnO_2 to regenerate Sn at Ceramic Separator/Anode Inlet interface: (R₃)



The details of the physio-chemical processes and the corresponding mathematical equations are presented in earlier reports and will not be discussed here.

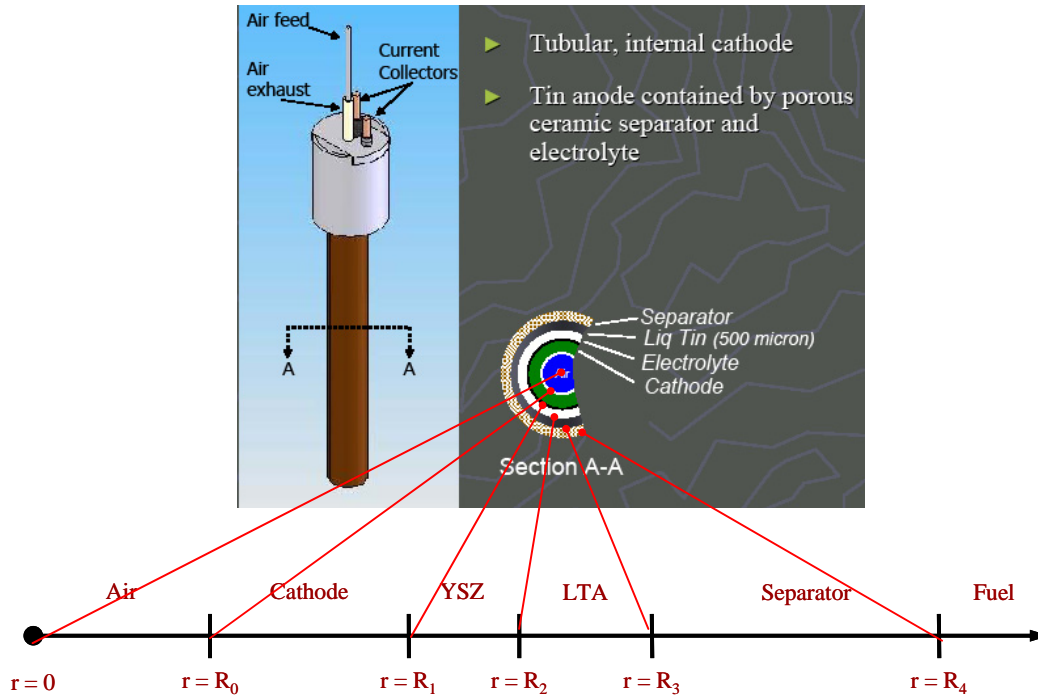


Figure 7. Projection of the tubular design of the LTA-SOFC system (developed by Cell Tech) to a one-dimensional axisymmetric modeling domain.

3.3.1.1 LTA-SOFC System with H₂ Fuel

The model equations were incorporated into Comsol Multiphysics and numerically solved for the cell voltages over a range of specified current densities. Figure 7 to

Figure 11 present various studies considering pure H₂ as anode fuel. Figure 8 presents the simulated polarization curve for the LTA-SOFC system along with the equilibrium curve for the system. The results reveal a drastic deviation from the equilibrium potential indicating huge polarization losses, especially at high current densities. The polarization losses corresponding to the individual cell components are presented in Figure 9. For the parameter values used in the simulation, polarization losses from anode, cathode and the electrolyte were found to be significant.

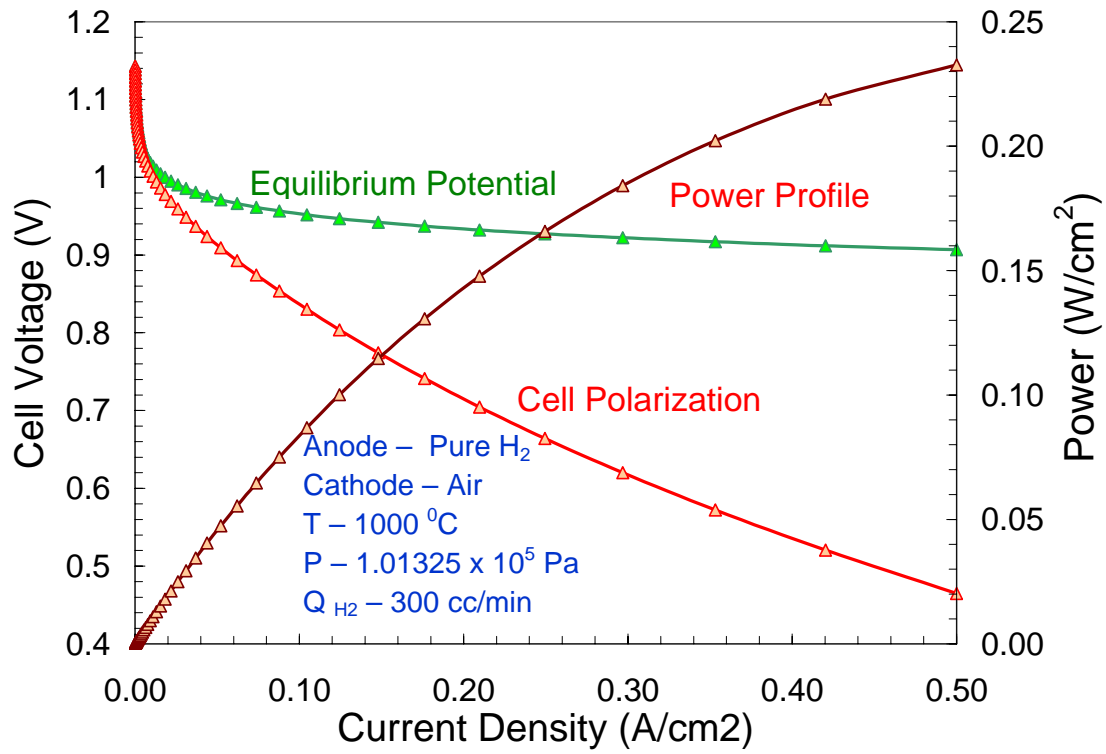


Figure 8. Plot showing the simulated polarization curve of the LTA-SOFC cell, along with the equilibrium potential of the system. The corresponding power profile is shown on the secondary y-axis. The system was simulated for H₂ and air as anode and cathode fuel respectively, operating at a temperature of 1000 °C. The anode fuel flow rate was fixed at 300 ccm.

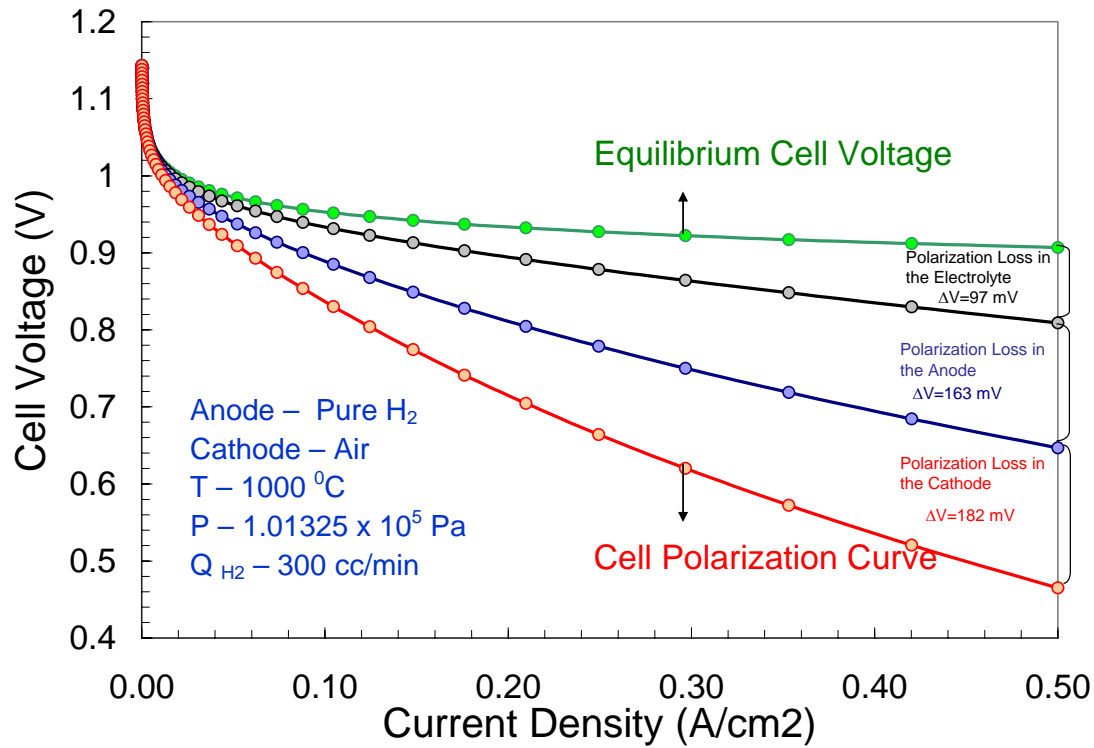


Figure 9. Plot showing the contribution of the anode, cathode and the electrolyte polarization towards the overall cell polarization at various operational current densities. The system was simulated for H_2 and air as anode and cathode fuel respectively, operating at a temperature of $1000^\circ C$. The anode fuel flow rate was fixed at 300 ccm.

Figure 10 shows the simulated mass fractions of the reactant and product species at the anode and cathode interfaces. The mass fraction of H_2O increases at higher current densities, as the cathode reaction rate increases, while the mass fraction of H_2 decreases at higher current densities owing to higher fuel consumption. The mass fractions of O_2 and N_2 were not affected by current density because air was always assumed to be available at the interface, i.e. the atmospheric mass fraction compositions of O_2 and N_2 were fixed at the air/cathode interface ($r=R_0$).

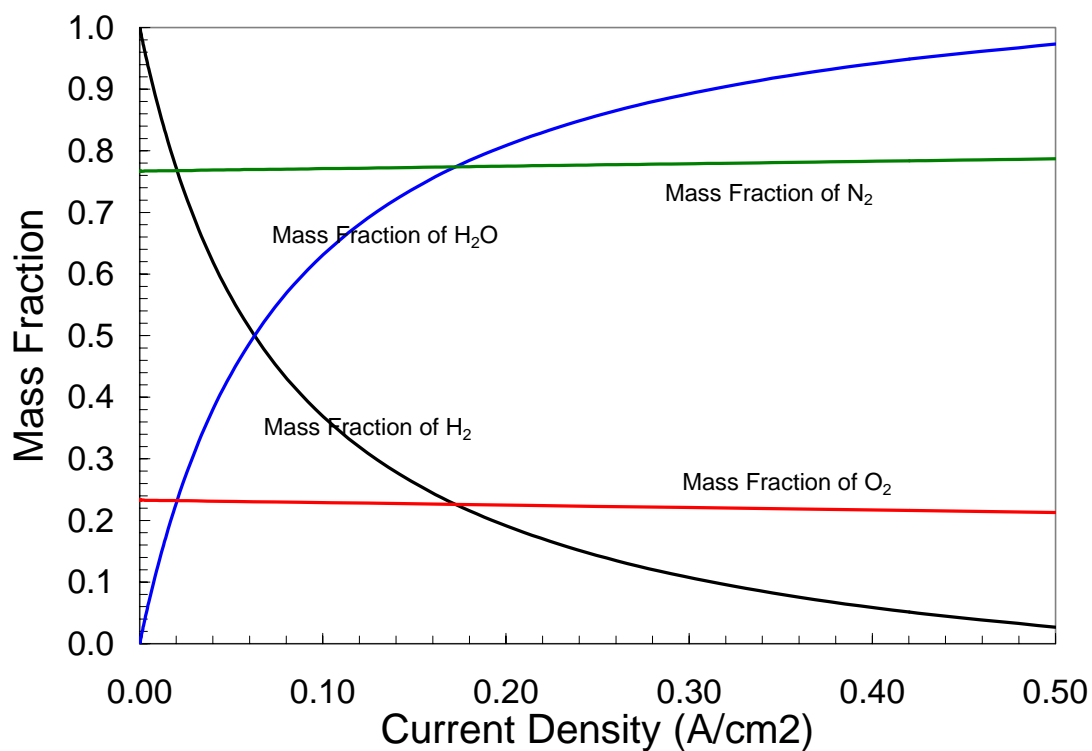


Figure 10. Plot showing the composition of the anode/cathode reactants and products at various operational current densities. The mass fractions of anode constituents i.e. H₂ and H₂O were evaluated at the separator/LTA interface (R₃), while the mass fractions of the cathode constituents i.e., O₂ and N₂ were evaluated at the cathode/electrolyte interface (R₁).

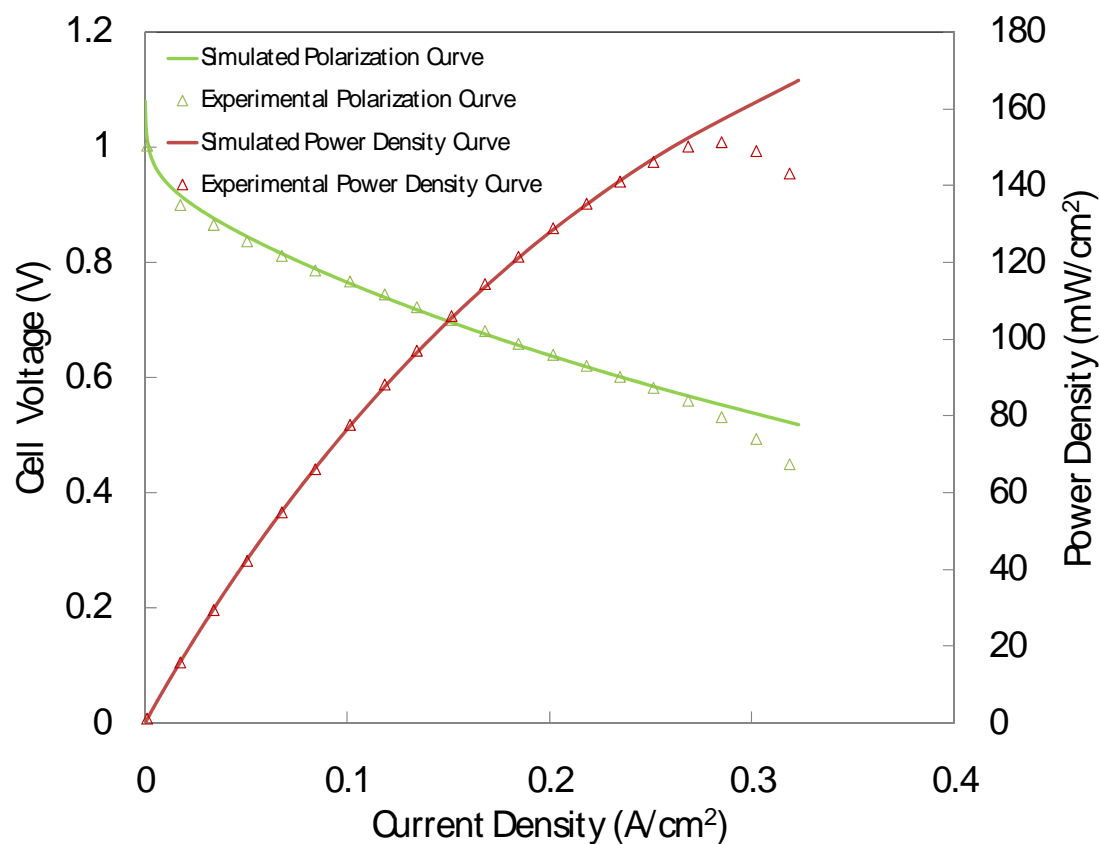


Figure 11. Plot showing the comparison of the polarization and power density predictions from the LTA-SOFC model developed at USC to the experimental data obtained on the tubular LTA-SOFC cell at Cell Tech. The cell was operated with H_2 as anode fuel and air as cathode fuel, at a cell operating temperature of $1000^\circ C$. The anode fuel flow rate was set at 300 sccm.

Figure 11 presents the comparison between the numerical predictions and the experimental data obtained on the Gen 3.1 LTA-SOFC cell at Cell Tech. The simulated polarization curve shows good agreement to the experimental data almost over the entire range of current densities. However at very high current densities ($> 0.3 A/cm^2$), additional polarization losses were observed in the experimental data than predicted by the model. The origin of these additional polarization losses at very high current densities is not clear at this moment and is subject to further investigation. Initial case studies indicate that low cathode pressure might be a possible source for these polarization losses.

3.3.2 LTA-SOFC System with CO/H₂ Fuel Mixture & CH₄/CO/H₂ Fuel Mixture

The previously described model was extended to accommodate CO/H₂ mixture as anode inlet fuel. Consequently the unknown mass fractions to 4 different species have to be solved for using Stefan-Maxwell's relation in the anode separator region. No significant change in the polarization behavior (not shown) was observed when the fuel mixture was changed from H₂ to CO anode fuel. Figure 12 shows the mass fractions of the four species in the separator/LTA interface. The plot predicts a higher consumption of fuel species (H₂ and CO) indicated by the low values of mass fraction at higher operating current densities, and increased water generation. Figure 13 shows the predicted mass fractions for various anode fuel constituents when a CH₄/CO/H₂ mixture was used as inlet fuel. Here again, there was no significant difference in the polarization behavior that was observed compared to the case of pure H₂ as anode fuel.

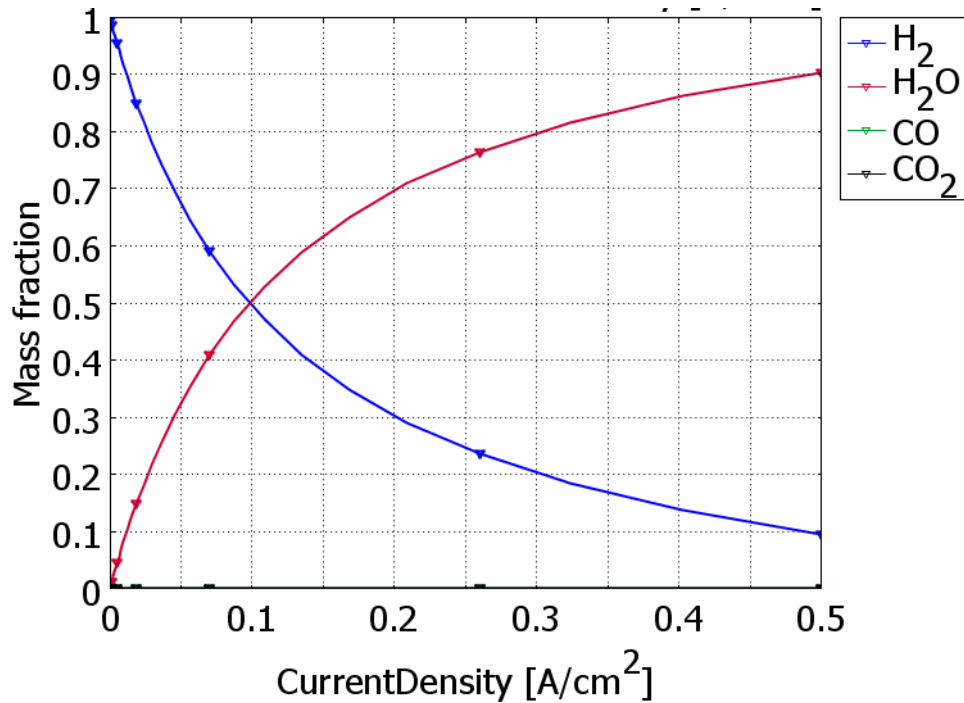


Figure 12. Plot showing the mass fraction of H₂, H₂O, CO and CO₂ in the separator (anode)/LTA interface (R₃) as a function of operation current density. The cell was operated under H₂/CO mixture (99/1 mol%) as anode fuel and air as cathode fuel. The anode inlet flow rate was fixed at 1000 sccm. The values for current densities chosen were 50 points logarithmically spaced between 10⁻⁴ A/cm² and 0.5 A/cm² [Note, that the mass fractions of CO and CO₂ are very low compared to H₂ and H₂O, and lie along the x-axis]

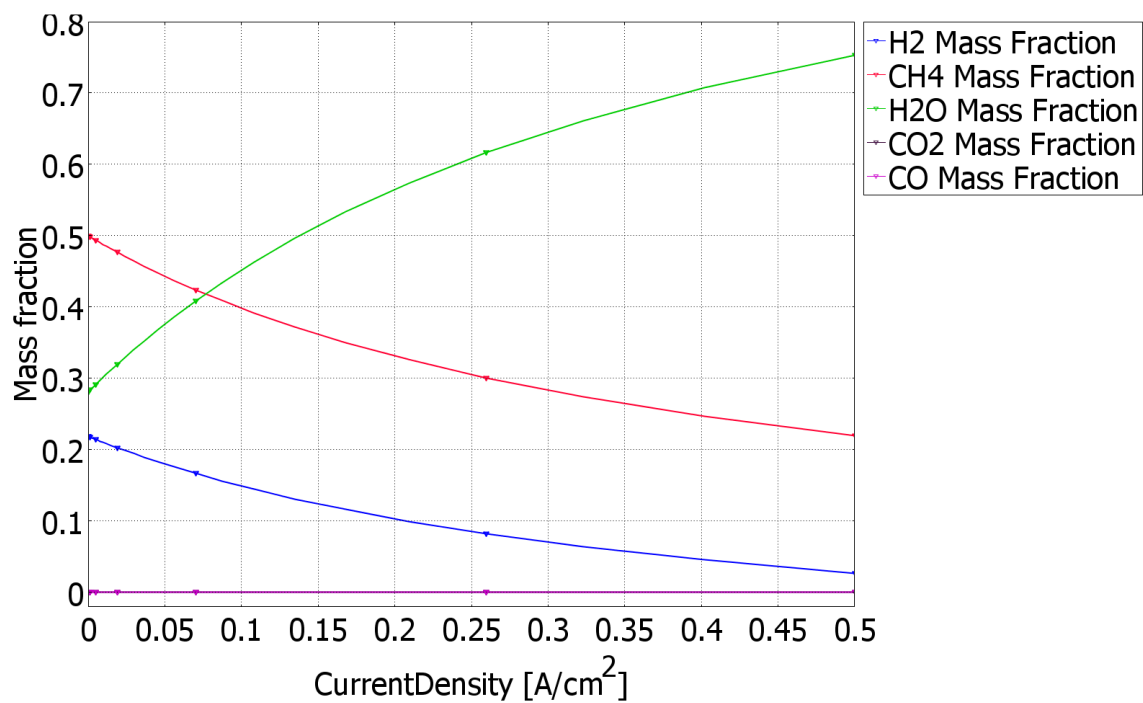


Figure 13. Plot showing the mass fraction of H₂, CH₄, H₂O, CO and CO₂ in the separator (anode)/LTA interface (R₃) as a function of operation current density. The cell was operated under 80/19.99/0.01 mol% mixture of H₂/CH₄/CO as anode fuel and air as cathode fuel. The anode inlet flow rate was fixed at 1000 sccm. The values for current densities chosen were 50 points logarithmically spaced between 10⁻⁴ A/cm² and 0.5 A/cm² [Note, that the mass fractions of CO and CO₂ are very low compared to H₂ and H₂O, and lie along the x-axis]

3.3.3 Effect of Parameters on LTA-SOFC Cell Performance

Case studies were done to understand the effect of various parameters on the polarization behavior of the LTA-SOFC system. The effect of electrolyte thickness, cathode porosity, cathode air pressure, and anode exchange current densities are shown in Figure 14 through Figure 17 respectively. While the effect of cathode porosity was minimal, the other parameters strongly affected the polarization behavior. The effect of electrolyte thickness was more pronounced at higher operating current densities, lowering the polarization plateau. As expected, thinner electrode suffered from lesser polarization losses.

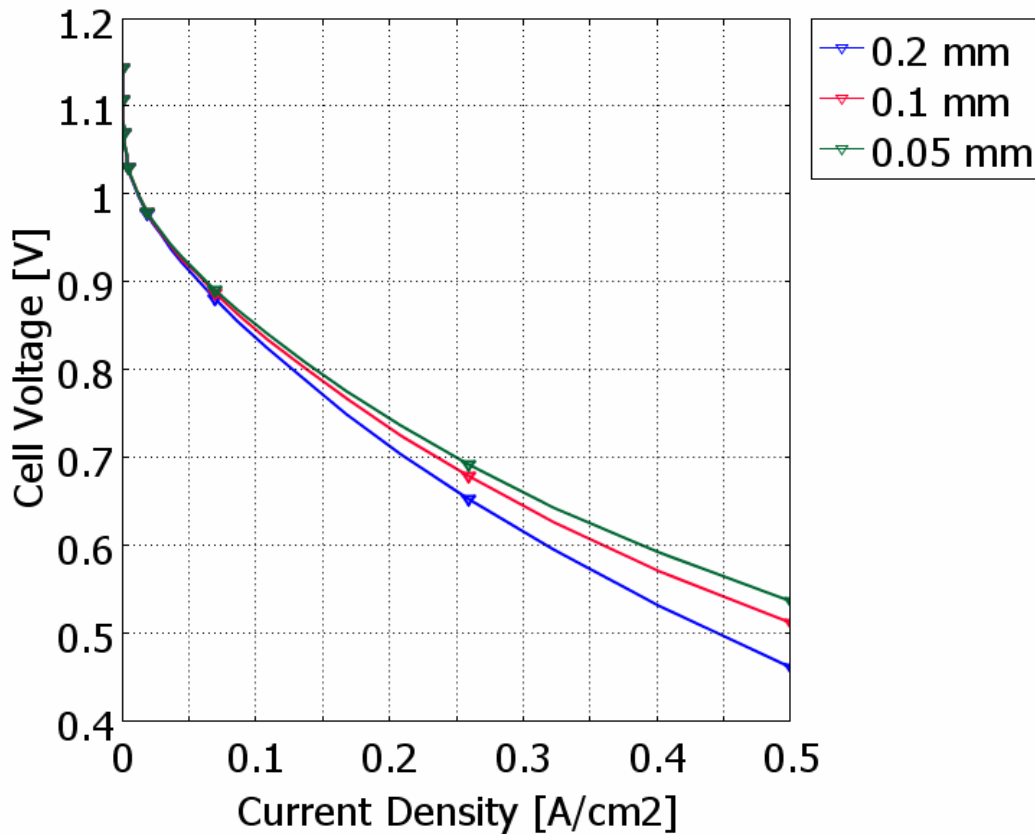


Figure 14. Plot showing the effect of YSZ Electrolyte Thickness ($R_1 < r < R_2$) on Cell Polarization Behavior of the LTA-SOFC System. The cell was operated with H_2 as anode fuel and air as cathode fuel, at a cell operating temperature of $1000^\circ C$. The anode fuel flow rate was set at 1000 sccm. The polarization curve was obtained by solving for the cell voltage for 50 logarithmically spaced current densities between $10^{-4} A/cm^2$ and $0.5 A/cm^2$

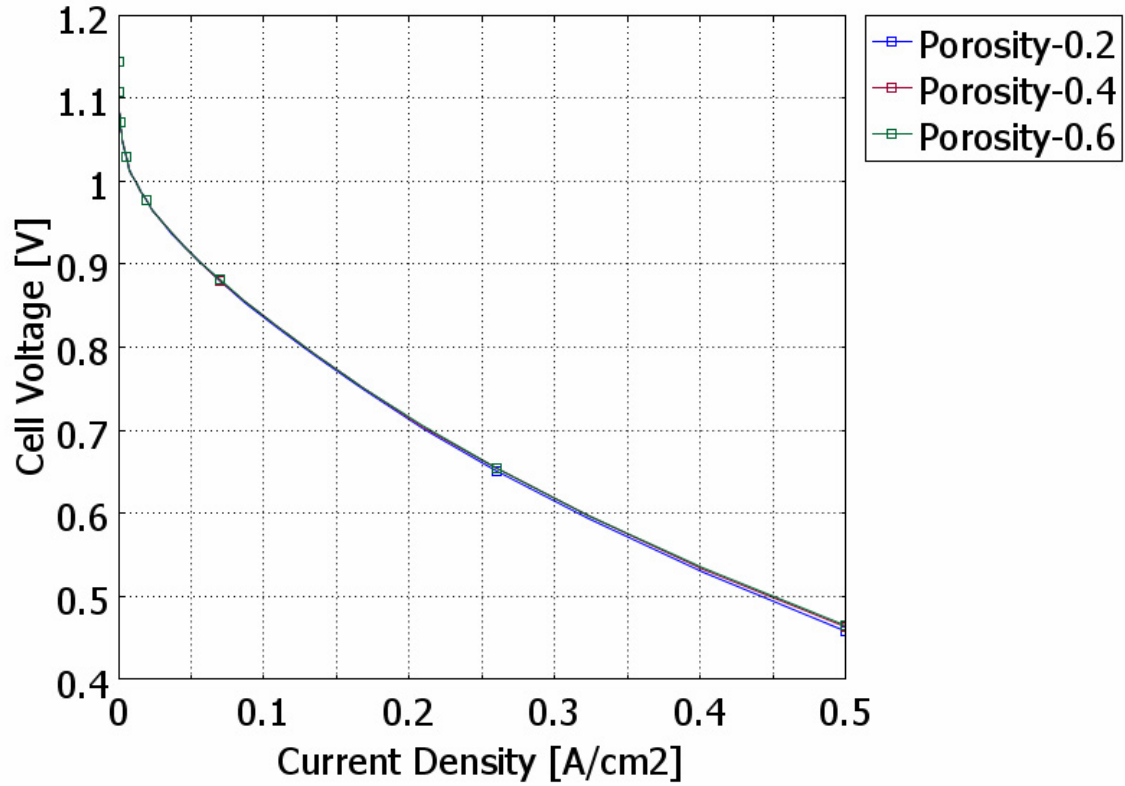


Figure 15. Plot showing the effect of Cathode Porosity on Cell Polarization Behavior of the LTA-SOFC System. The cell was operated with H_2 as anode fuel and air as cathode fuel, at a cell operating temperature of $1000^\circ C$. The anode fuel flow rate was set at 1000 sccm. The polarization curve was obtained by solving for the cell voltage for 50 logarithmically spaced current densities between $10^{-4} A/cm^2$ and $0.5 A/cm^2$

The cathode inlet pressure has a strong effect on the polarization behavior of the cell. Low pressure operation creates higher concentration polarization in the electrodes at high current densities resulting in poor performance. At an operation pressure of 1psi, the cell was not able to yield any significant voltage beyond 0.2 A/cm²

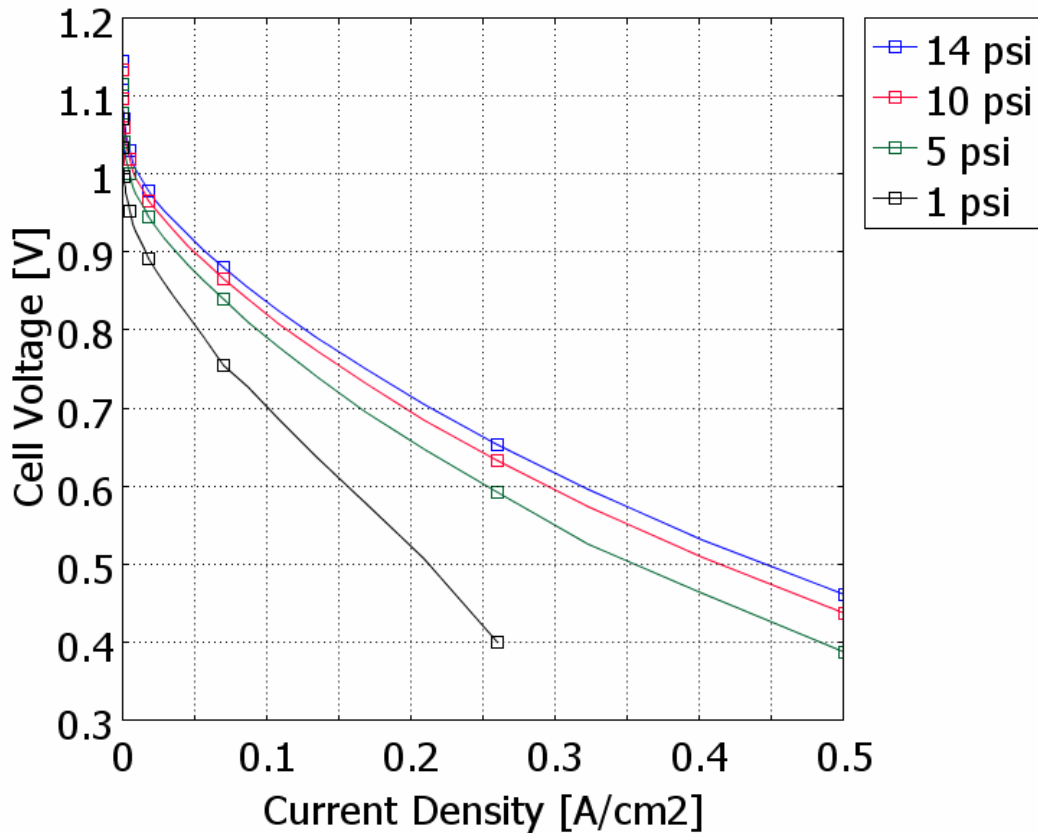


Figure 16. Plot showing the effect of Cathode Inlet Pressure on Cell Polarization Behavior of the LTA-SOFC System. The cell was operated with H₂ as anode fuel and air as cathode fuel, at a cell operating temperature of 1000 °C. The anode fuel flow rate was set at 1000 sccm. The polarization curve was obtained by solving for the cell voltage for 50 logarithmically spaced current densities between 10⁻⁴ A/cm² and 0.5 A/cm²

The effect of anode exchange current density on the polarization behavior is presented in Figure 17. A value of 1200 A/m² was used for all of the previous simulations. This plot shows marginal improvement in polarization performance at even higher values for anode exchange current densities. However, at low values of exchange current densities, the cell suffered from severe kinetic losses, as observed from the overall drop in the polarization behavior over the entire range of current densities.

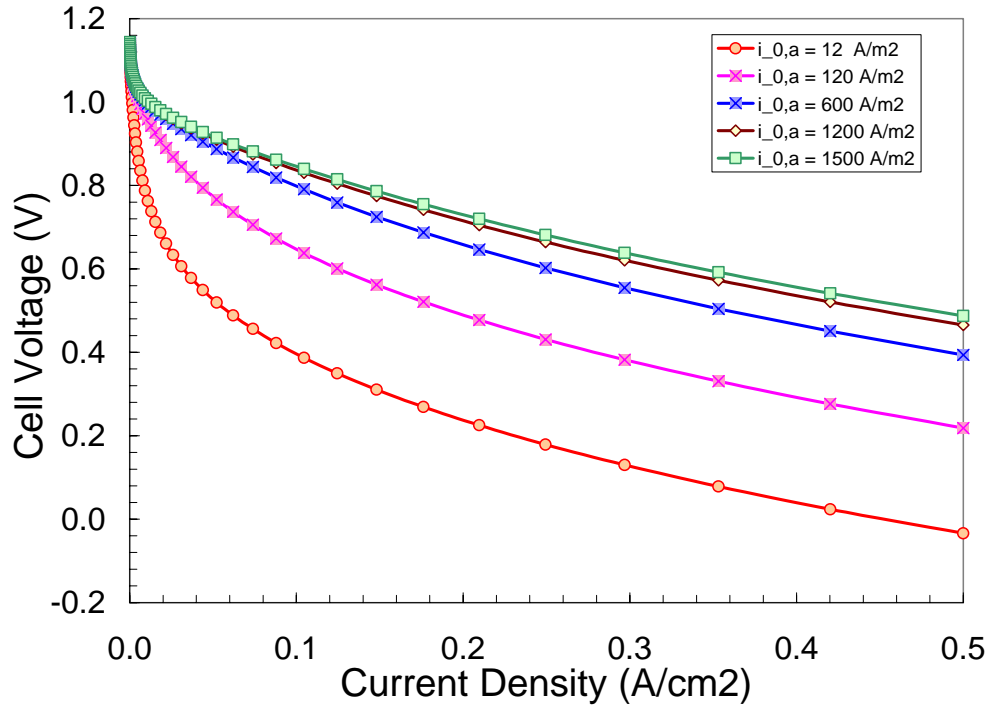


Figure 17. Plot showing the effect of anode exchange current density on Cell Polarization Behavior of the LTA-SOFC System. The cell was operated with H₂ as anode fuel and air as cathode fuel, at a cell operating temperature of 1000 °C. The anode fuel flow rate was set at 1000 sccm. The polarization curve was obtained by solving for the cell voltage for 50 logarithmically spaced current densities between 10⁻⁴ A/cm² and 0.5 A/cm²

3.3.4 Transient Model for the LTA-SOFC Cell

Although typical fuel cell systems reach to a steady state operation at very short times, the transient behavior in this system is of critical importance especially at start up and shut down times. In addition, there is also a short transient behavior under normal operating temperatures when a current is impressed from open circuit conditions. Figure 18 shows the predicted transients in the voltage for various values of current densities as marked. The cell was initially at open circuit conditions (~ 1.2 V) and the corresponding current density was applied to the system. For the case of high current densities, a monotonic drop in cell voltage was observed before reaching a steady state, while for the case of low current densities, the cell voltage dropped initially, followed by a gradual increase before reaching a steady state. The observed transience at high current densities is due to the diffusion limitations in the anode fuel, while at low current densities the diffusion in LTA dominated the transient behavior.

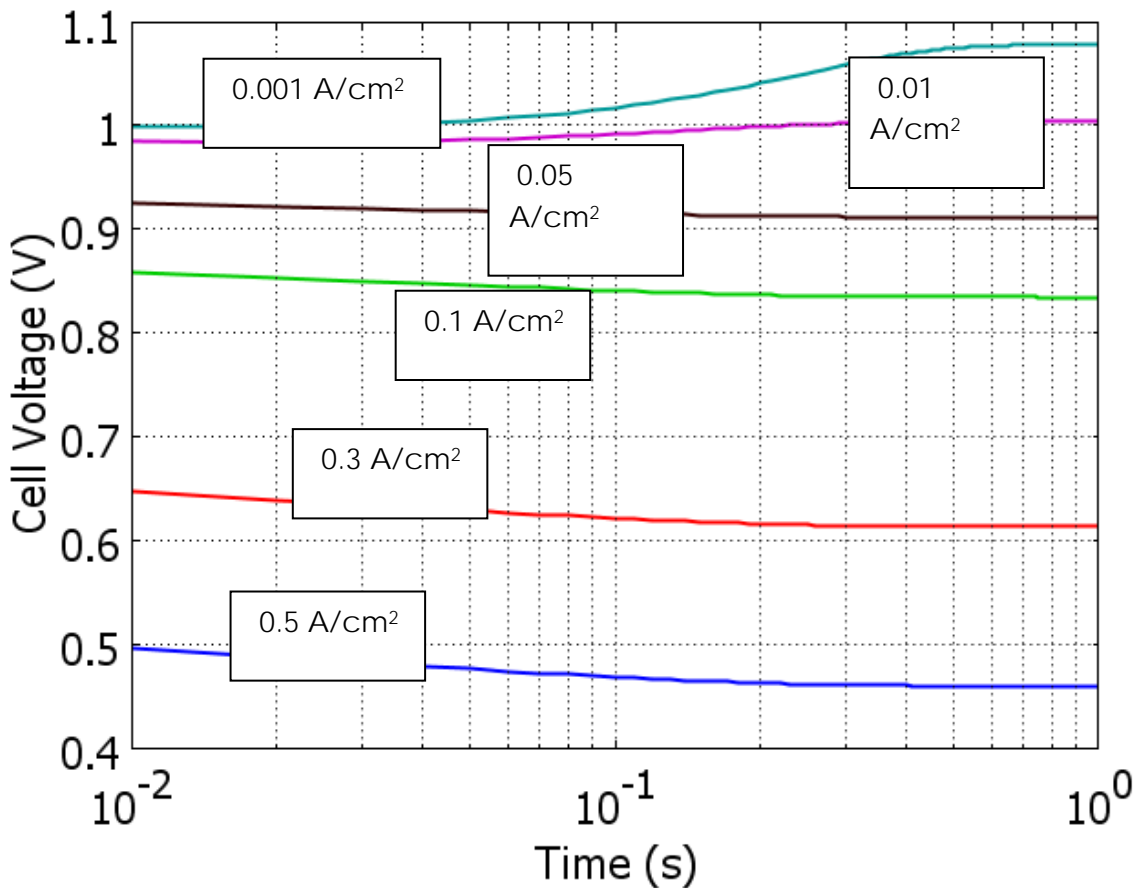


Figure 18. Plot showing the transience in the cell voltage of the LTA-SOFC system (on a logarithmic time axis) for different values of current densities as shown in the plot. The cell was operated under 80/19.99/0.01

mol% mixture of $H_2/CH_4/CO$ as anode fuel and air as cathode fuel and the anode inlet flow rate was fixed at 1000 sccm.

3.4 Conceptualization of a 500 W liquid-metal anode fuel cell system

3.4.1 US Army Mission Needs

Information is presented in this section regarding both the CERDEC Army Power Division and Anticipated Army Battery and Battery Charger Needs. The information contained herein represent's MS2's best understanding of information which is subject to change and possible alternative interpretation. Anticipated Army Battery and Battery Charger Needs

Battery Chargers in the 500W range serve an important US Army need. The fuel cell power requirement is driven by the Army need to recharge 4 specific 50W batteries in 2 hours or less.

Soldiers operating at the Squad level utilize Small Squad Radios to provide individual communications. These Small Squad Radios operate over a range of 5-10 kilometers, which require one 50W battery per radio. It should also be noted that the radios can be operated on either primary or secondary batteries. Primary batteries are typically disposable and used in situations not amenable to recharging (i.e., intense combat situations, etc). Secondary batteries are typically rechargeable and used in situations where recharging operations are possible.

The Small Squad Radio is powered by Radio Battery BB-2590 (made by Bren-Tronics, see Figure 19. The BB-2590 is a rechargeable lithium-ion battery certified for military use. It has a total power of 207 W-hrs and is utilized in various radios, including SINCGARS (Single Channel Ground and Airborne Radio System).



Figure 19: BB-2590 Radio Battery

BB-2590 batteries can be recharged using a Soldier Portable Charger (SPC), such as Battery Charger PP-8498 (made by Bren-Tronics, see (Figure 20). The SPC is a state of the art portable battery charger designed for field or depot use and accepting AC or 28V DC power. It is capable of charging 8 batteries (2 simultaneously with 6 batteries in queue) in 8 hours or less with easy to follow LED lighting sequences. This charger will charge and maintain a variety of batteries using an appropriate mating adapter.

The portable charger shown in Figure 20 is outfitted with an adapter, in this case Adapter J-6358 (Bren-Tronics, see Figure 21). Utilizing adapters (referred to as "shoes") allows standard charging of various batteries. Adapter J-6358 holds 2 batteries.



Figure 20: PP-8498 Battery Charger



Figure 21: J-6358 Battery Charging Adapter

Squad level charging equipment in the 500W range provides the capability to recharge batteries for multiple soldiers simultaneously. Given the expected size and weight for this scale charger, it is not expected that this unit will be carried by soldiers for extended periods of time, but rather transported in military vehicles utilized at the squad level (HMMWV, personnel carrier, tank, truck, etc). In addition to providing the means to transport the fuel cell battery charger along with other necessary squad equipment, these military vehicles also provide a source of JP-8 needed to operate the fuel cell

unit. When in use, it would be expected to be hand carried by 1 or 2 soldiers for short distances.

Directive 4140.25 established the US military's "one fuel forward" policy designating JP-8 as the single operating fuel for all military forward deployed equipment. In the U.S. military, JP-8 is used in the engines of nearly all tactical ground vehicles and electrical generators. The M1 Abrams series of battle tanks also uses JP-8 fuel in its gas turbine engine. The use of a single fuel for most combat applications greatly simplifies the wartime logistics system. The utilization of JP-8 in the LTA-SOFC battery charger, without desulfurization and other pre-treatment capitalizes on a widely available military fuel source and provides a unit that does not complicate logistics. While the Army has identified alternative fuel cell applications using other fuel sources, such as methanol, these are mostly for unique applications and will not gain the wide use expected of JP-8. In fact, there may be long term possibilities for the military to adopt either permanently or semi-permanently mounted JP-8-powered fuel cells within military vehicles, fully integrated with the vehicle's fuel and battery systems to provide squad level battery recharging. As military battery charger power requirements grow, as expected, to the 1 kW level or above, these vehicle mounted options will become even more plausible.

In addition to recharging batteries, the JP-8-fueled fuel cell can operate as a battery itself, giving it broader versatility. Given the expected low noise feature, whether operating as a fuel cell or battery, the LTA-SOFC presents additional options for Army Silent Watch applications, where it is essential to maximize energy and minimize weight and volume. This capability should be explored through successively larger stack testing to demonstrate the ability to power silent watch operation for an extended period of time.

3.4.2 System Conceptual Design

This section addresses four topics. Initially, it presents System Requirements driving the conceptual design. Secondly, a high level system flow diagram with description is presented. The third section provides the details of the system conceptual design for the JP-8-fueled LTA-SOFC 500W Battery Charger being proposed. The final section describes potential future trade studies that could be conducted to optimize various aspects of the system design.

3.4.2.1 System Requirements

Utilizing information contained in the STTR description and obtained from CERDEC, a set of system level requirements has been developed. Requirements are categorized as relating to Recharger Performance (performance standards which the system must meet), Physical (Weight and Volume) and Operational (how and under what

conditions the system must operate). All requirements are summarized below in Table 3.4.2-1 .

	<i>Metric</i>	<i>Units</i>	<i>Comment</i>
Recharger Performance			
# of battery recharged	4	per charger	simultaneously
Recharging time	2	Hrs	
Battery Type	BB-2590		Possibly adapt for others
Secondary Battery Types	BB-390, BB-2847, BB-2800, LW-SI, Future Force		IAW CERDEC draft charger spec
Output Power	500	W	
Output Voltage	22-28	V	Output voltage of SPC PP-8498
Cell Efficiency	30	%	
System Efficiency	25	%	
Physical Requirements			
Weight (Dry)	10	Kg	IAW CERDEC draft charger spec
Volume	20 – 50	Liters	
Operational Requirements			
Fuel Cell fuel	JP-8		CERDEC SITR
Startup Time	10	Min	IAW CERDEC draft charger spec
Lifetime	5,000	Hrs	IAW CERDEC draft charger spec
Fuel Consumption Rate	0.26	Liters/min	IAW CERDEC draft charger spec
Operating Temperature Range	-32 to +49	°C	IAW CERDEC draft charger spec
Storage Temperature Range	-33 to +71	°C	IAW CERDEC draft charger spec
Altitude Range	1525	M	IAW CERDEC draft charger spec
System Noise	MIL-STD-1474D (30 ft)		IAW CERDEC draft charger spec
Shock	MIL-STD-810F		IAW CERDEC draft charger spec
Vibration	MIL-STD-810F		IAW CERDEC draft charger spec

Table 3.4.2-1: System Requirements

3.4.3 System Level Flow Analysis

A preliminary high-level system flow analysis has been conducted. This analysis included the development of a system level Process Flow Diagram (PFD), as shown in Figure 22 and an analysis of conditions at key points throughout the system. Key points where flow conditions were analyzed are indicated as stream markers (Sx) in Figure 22 and summarized in Table 3.4.3-1. The components used in the diagram are described in further detail in Section 3.4.4. A mass balance analysis was conducted to characterize preliminary mass flows throughout the system. Detailed design is required to establish pressure drops across components, blower/pump sizing, heat exchanger sizing, and ducting losses.

Inputs to the system include JP-8 liquid fuel and ambient air. The inlet air is drawn in at S1, and is represented by a blue flow line. The system level air flow rate was determined using a per cell air flow rate of 300 cc/min. A 500W stack consisting of 200 cells requires a flow rate of 40 liters/min. Similarly, the inlet liquid fuel flow (depicted as a black flow line) is governed by the required per cell fuel flow rate of 50 microliter/min and a stack flow rate of 0.216 liters/hr. For the purpose of this high level analysis, it is assumed that both fuel and air are being drawn into the system at ambient conditions (30°C and 1atm).

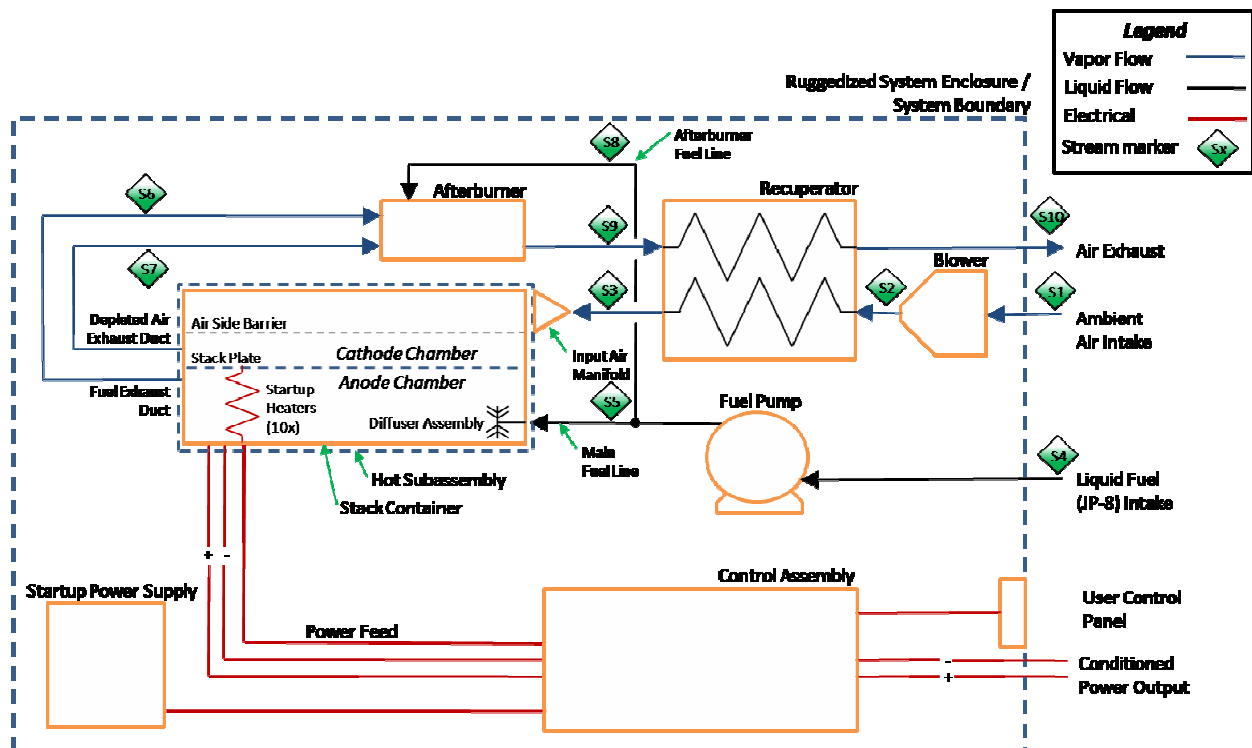


Figure 22: System Level Flow Diagram

The inlet air flow rate remains constant through the Blower (S2), which elevates the pressure sufficiently to proceed through the system and the Recuperator (S3), which pre-heats the air prior to entering the Hot Subassembly.

The liquid fuel is pumped into the system and distributed to the Hot Subassembly via the Diffuser Assembly (S5). A small portion of the inlet fuel flow is diverted to the Afterburner (S8) to combust the mixed exhaust gas. As an initial estimate, the mass of the fuel diverted to the afterburner is assumed to be negligible for this analysis.

Depleted air (S7) and fuel exhaust (S6) exit the Hot Subassembly at approximately 1000°C and are combined in the afterburner, where they are combusted with makeup fuel supply. Afterburner exhaust (S9) passes through the Recuperator to pre-heat the inlet air. System exhaust (S10) is dispelled from the system above 100°C to prohibit condensation within exhaust lines.

Finally, power harvested from the Hot Subassembly is sent to the Control Assembly for Power Conditioning and subsequent distribution.











Stream Marker (see Figure 22)	Temp (°C)	P (atm)	ρ (kg/m ³)	\dot{m} (kg/hr)	Constituents
	30	1	1.1614	2.7874	Air
	30	2.75	1.1614	2.7874	Air
	900	2.5	0.2950	2.7874	Air
	30	1	800	0.1728	JP-8
	30	2.5	800	0.1728	JP-8
	1000	2	800	0.1728	JP-8
	1000	2	0.2750	2.7874	Air
	30	1.1	≈ 0	≈ 0	JP-8
	1500	1.75	0.1950	2.9602	Air & JP-8
	120	1.25	0.8711	2.9602	Air & JP-8

Table 3.4.3-1: High-Level Mass Balance Analysis

3.4.4 Conceptual Drawings/Diagrams

The system concept presented here describes a 500 W portable system fuel cell battery recharger which integrates the Gen 3.1 fuel cell and utilizes JP-8 as a fuel without reforming or fuel processing. As described previously, the unit has two inputs (air and fuel) and outputs in the form of exhaust products and power for recharging. The overall system has been subdivided into subsystems, which include the following:

- Cell and Stack Assembly
- Hot Subassembly
- Fuel Delivery Assembly
- Exhaust Air Assembly
- Intake Air Assembly
- Control Assembly/Power Conditioning Unit
- Enclosure Assembly

The system description provided here starts with the individual fuel cell, and sequentially builds the system, subsystem by subsystem. Note that the conceptual design presented has not been optimized for size, weight, ruggedization, or any other consideration.

3.4.4.1 Cell and Stack Assembly

The proposed battery charger is based around CellTech's Gen3.1 Fuel Cell as shown in Figure 23. There are two air ports on the top of the cell, one for Intake Air and one for Exhaust Air. For proper integration of this cell into the final assembly, the Intake Air port is required to extend higher than the Exhaust Air port, as will be demonstrated in Section 3.4.4.4. Additionally, there are two current collectors on the top of the fuel cell that connect to the anode and cathode sides of the fuel cell.

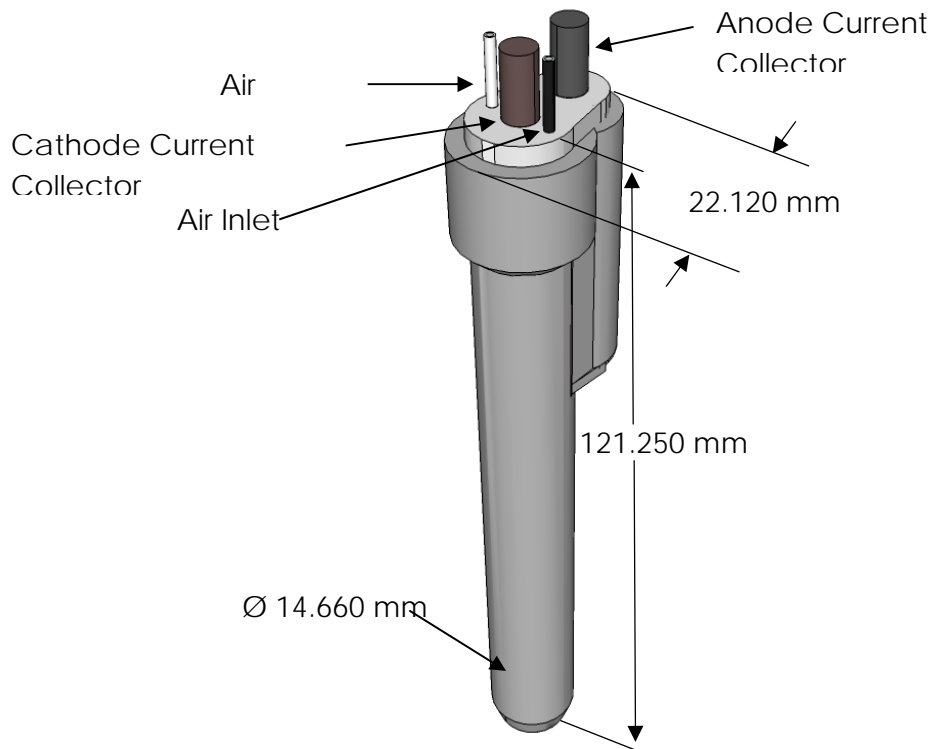


Figure 23: CellTech Gen3.1 Fuel Cell

Two hundred Gen3.1 Fuel Cells are used to form the cell stack. The total number of cells within the stack is driven by the per-cell power output plus projected margins necessary

to produce the required 500W battery charger output. Individual cells are held in place using the Stack Plate shown in Figure 24. Additionally, the Stack Plate provides structural stability to the cell stack, and a barrier between the fuel side gases and the depleted air exhaust.

The power drawn from each cell is collected via the Cell Power Interconnects. In order to meet system voltage and power requirements, twenty cells are linked in series to form a sub-stack. The output power from the ten sub-stacks is collected in parallel and is taken to the Control Assembly for power conditioning and distribution.

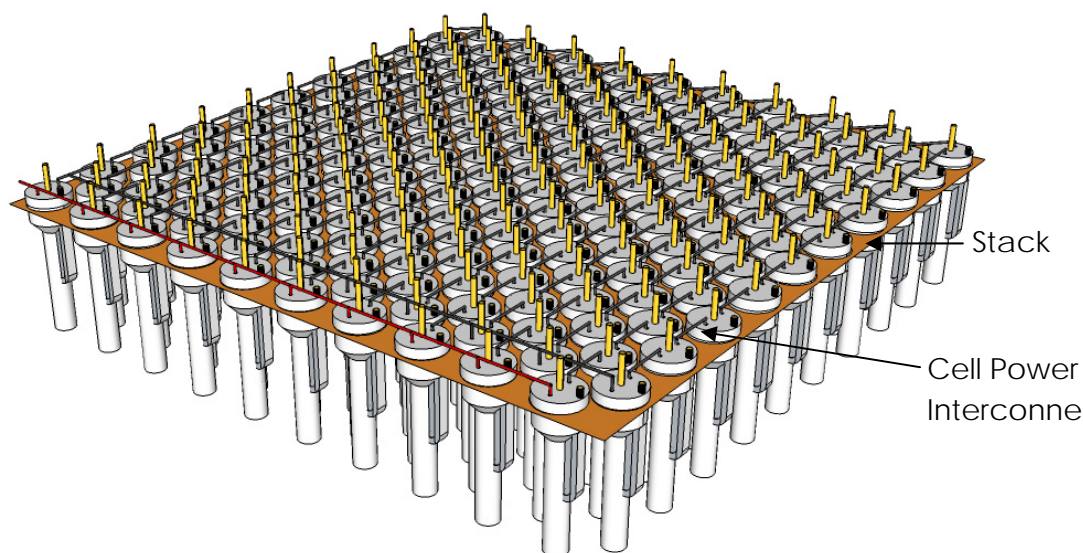


Figure 24: Cell Stack Assembly

3.4.4.2 Hot Subassembly

The Hot Subassembly houses the Cell Stack Assembly, directs flows to and from the proper regions of the Cell Stack and contains Cell Stack heat (see Figure 25). The Stack Container houses the Cell Stack Assembly. The container is responsible for containing the heat and gases required for proper fuel cell operation and ensuring that the various gases only interact as designed. Figure 25 shows the Stack Container. Fuel Exhaust Ports are located on either side of the Stack Container below the position of the Stack Plate to accommodate the removal of fuel-side products (i.e., unspent fuel, H_2O , CO_2 , and SO_2). A single Air Exchange Vent is positioned above the Stack Plate for the removal of depleted air. Finally, the Power Feed located on the exterior of the Stack Container is routed into the Control Assembly for power conditioning.

Air Exchange
Vent

Fuel Exhaust
Ports

Stack
Container

48

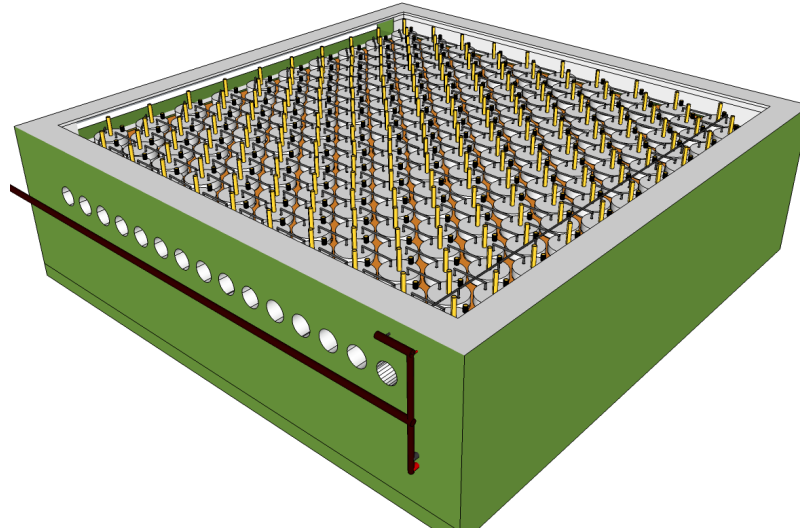


Figure 25: Stack Container Design

Figure 26 shows a cross-sectional view of the Hot Subassembly. As noted in Figure 26, the Stack Plate of the Cell Stack Assembly described previously separates the air and fuel sides of the fuel cell. The Startup Heaters raise the Hot Subassembly temperature to a point which supports spontaneous chemical reactions. Startup Heaters consists of ten electric resistance heating elements placed evenly between the rows of cells in the Cell Stack Assembly. It should also be noted that the Fuel Injector Nozzle Assembly is illustrated in Figure 26 but will be addressed in Section 3.4.4.3

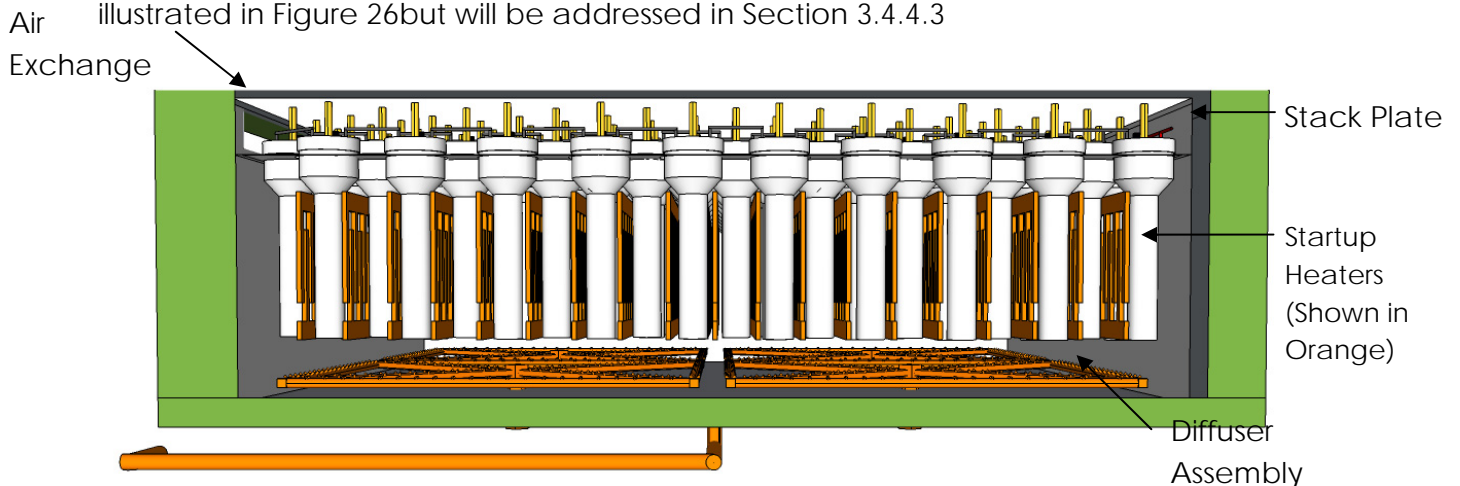


Figure 26: Section View of Hot Subassembly

3.4.4.3 Fuel Delivery Assembly

The Fuel Delivery System design is shown in Figure 27. Liquid fuel is drawn in from an external fuel source via a pump. From the pump exit, a small portion of the fuel flow is diverted to the Afterburner to support exhaust gas combustion (in Figure 27 this flow is depicted in the upward direction). The Main Fuel Line delivers the bulk of the inlet fuel to the anode side of the Hot Subassembly via a network of Injector Nozzles on the

Diffuser Assembly. Note that the Main Fuel Line is located outside the Hot Subassembly and the Diffuser Assembly is located within the Hot Subassembly as shown previously in

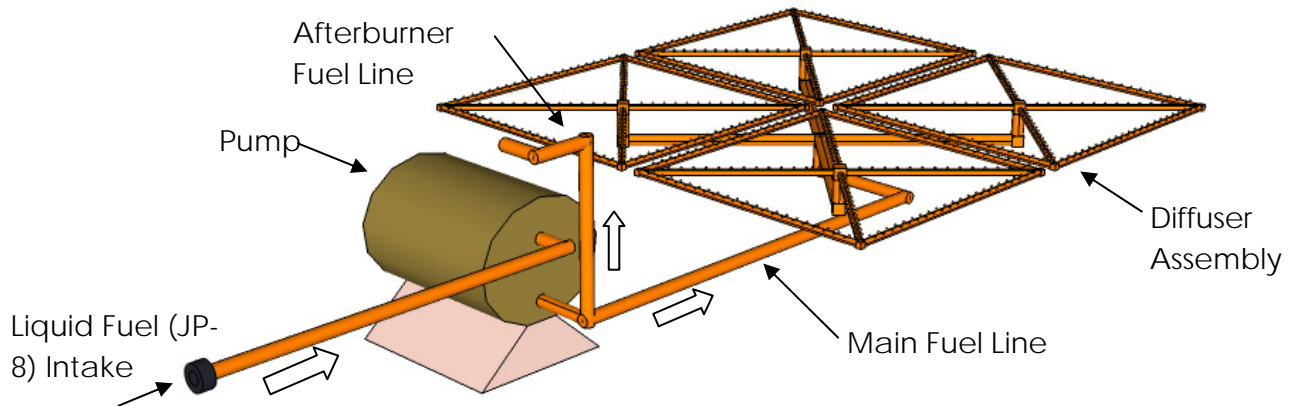


Figure 27: Fuel Delivery Design

Figure 28 shows a detailed view of the Diffuser Assembly. The placement, spacing, and orientation of the injector nozzles are designed to ensure even dispersion of vaporized JP-8.

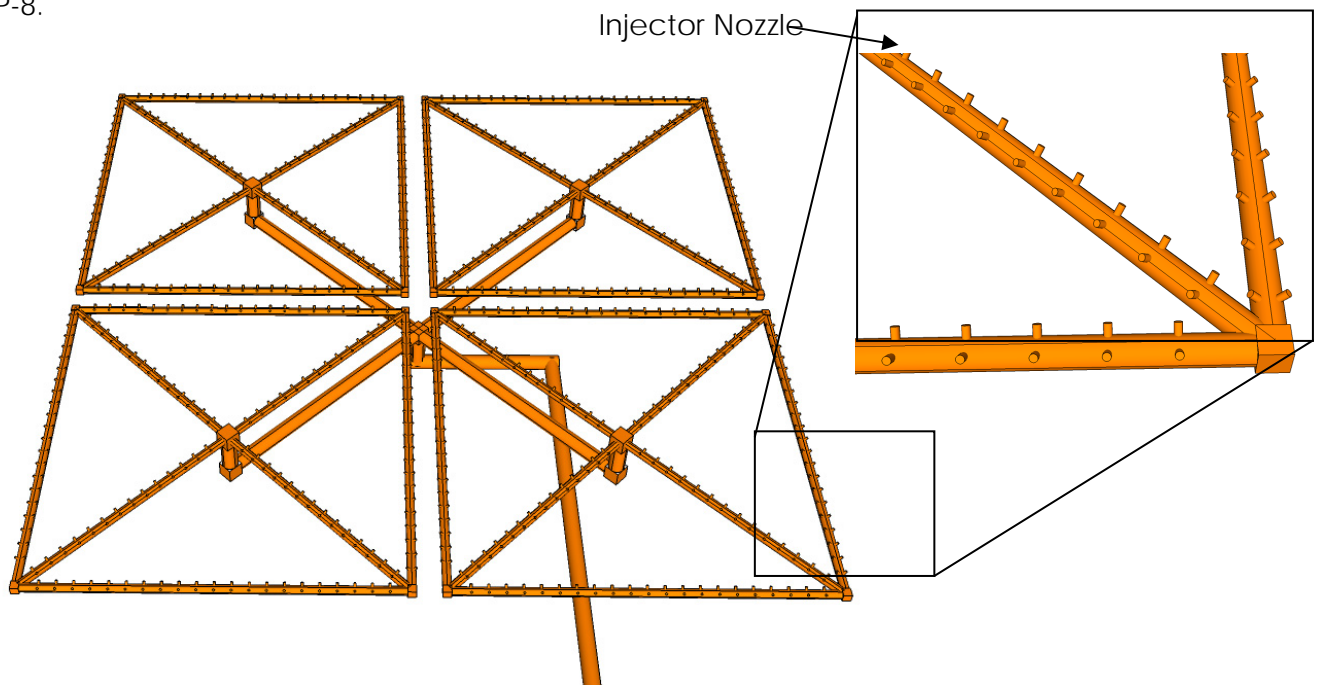


Figure 28: Diffuser Assembly Design

3.4.4.4 Exhaust Air Assembly

The Exhaust Air Assembly is shown in Figure 29. The Fuel Exhaust Ducts direct exhaust gases from the anode (fuel) side of the Stack Plate. Similarly, the Depleted Air Exhaust Duct draws the spent air from the top of the Hot Subassembly. These two exhaust gas flows are combined with fuel from the Afterburner Fuel Line and combusted in the Afterburner. Hot Afterburner products are then fed into the Recuperator, which is described in Section 3.4.4.5.

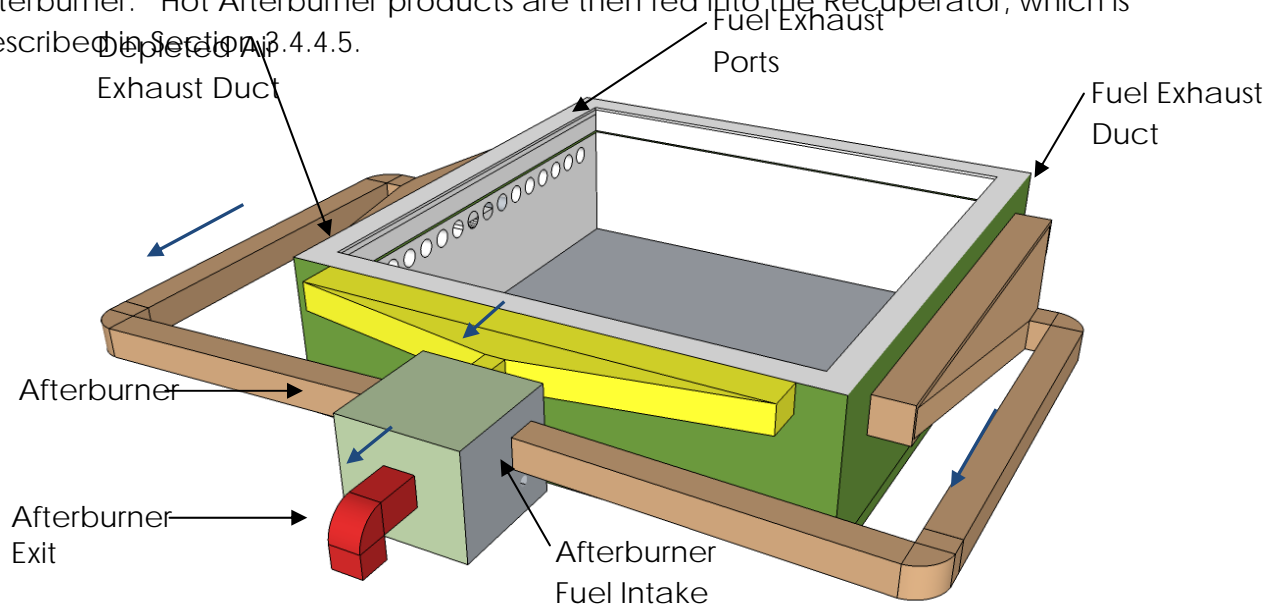


Figure 29: Exhaust System Design with Cell Stack Assembly Removed

3.4.4.5 Intake Air Assembly

The Intake Air Assembly is shown in Figure 30. Ambient air is drawn in via the Blower. Upon exiting the Blower the intake air passes through the Recuperator where it is heated indirectly by the hot exhaust. Upon exiting the Afterburner, the heated intake air is sent via ducting to the Input Air Manifold. The Input Air Manifold delivers the intake air to Fuel Cell Air Inlets for each cell and is designed to ensure even distribution of air to all cells.

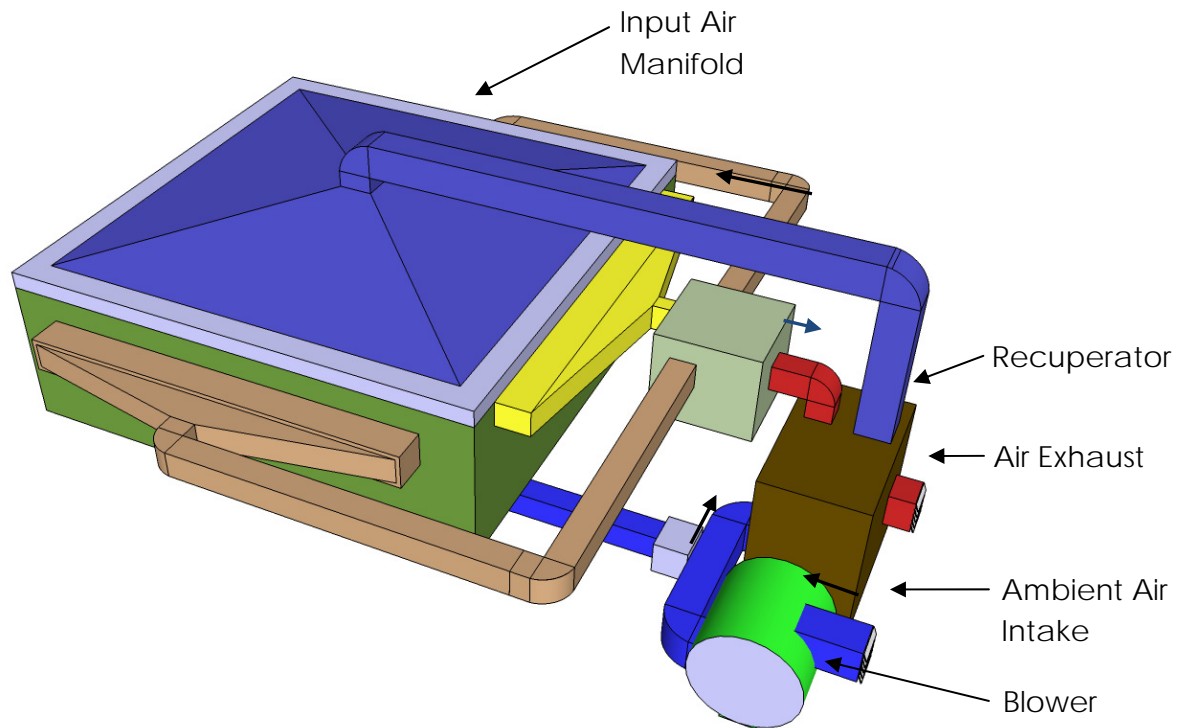


Figure 30: Air Intake and Delivery Subsystem

Intake Air is separated from Depleted Air by the Air Side Barrier (Figure 31). The intake air is transported to the fuel cells by the Fuel Cell Air Inlets that protrude through the Air Side Barrier. Additionally, the Air Side Barrier provides insulation between the Hot Subassembly and the rest of the system.

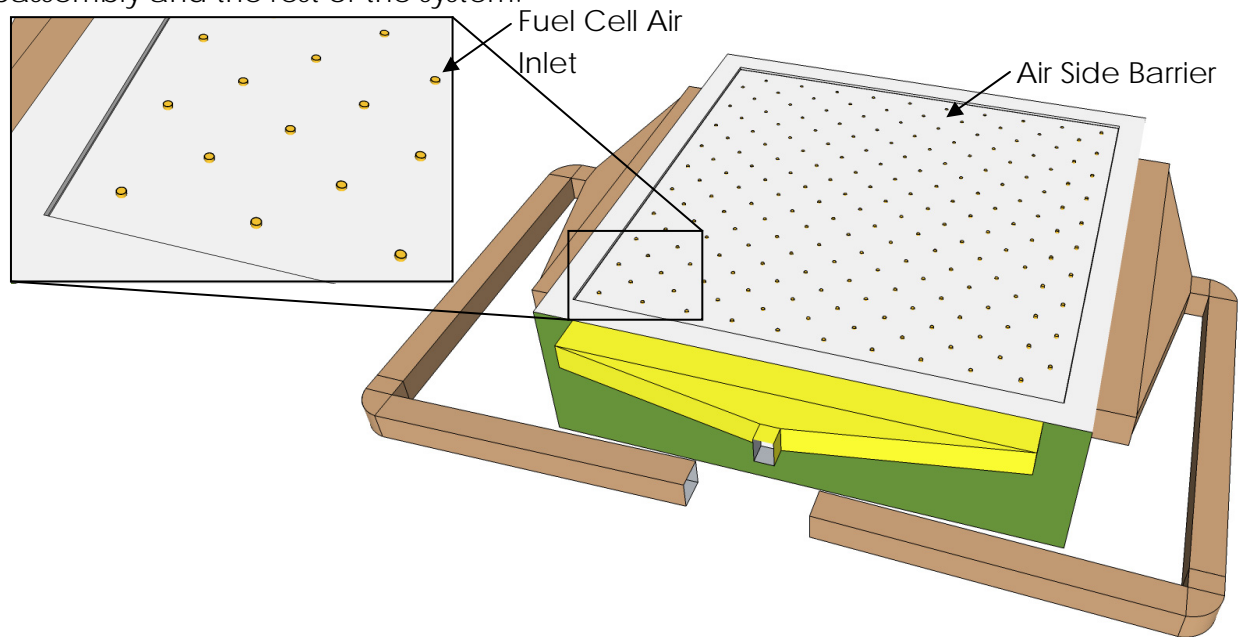


Figure 31: Air Side Barrier Design

3.4.4.6 Control Assembly / Power Conditioning Unit

The Control Assembly (Figure 32) is responsible for control and operation of the LTA-SOFC Battery Charger. The top level functions of the Control Assembly include:

- Startup/Shutoff switches and procedures
- Air temperature monitoring (pre/post Recuperator)
- Hot Subassembly temperature monitoring
- Flow rate monitoring/adjustment (air and fuel) for optimal power generation
- Fault Monitoring
- Output voltage/current regulation (power conditioning)

The User Control Panel of the Control Assembly includes start/stop/reset buttons, a simple display for charger status, access to fuses for easy replacement, and optional charging output jacks. Additionally, the Control Assembly includes an altimeter and ambient air thermometer for optimal flow regulation computations as well as regulators and capacitors for power conditioning.

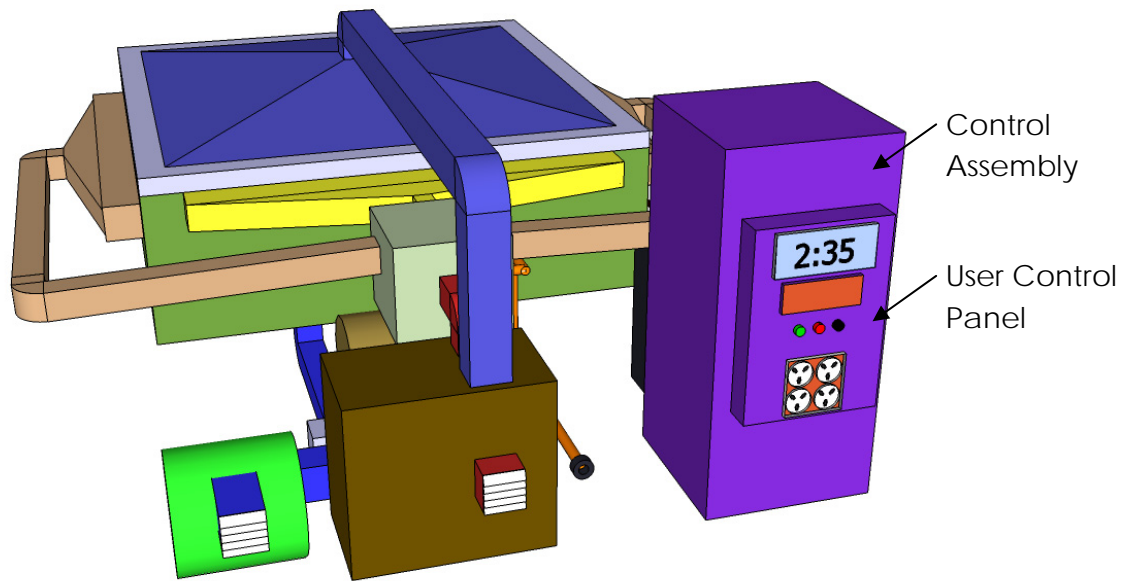


Figure 32: Control Assembly Design

Figure 33 shows a side view of the assembly. The Power Feed delivers the power created by the fuel cells to the Control Assembly for power conditioning and distribution. Additionally, the Startup Power Supply is an integrated rechargeable battery that provides power to the Control Assembly and Startup Heaters during system startup.

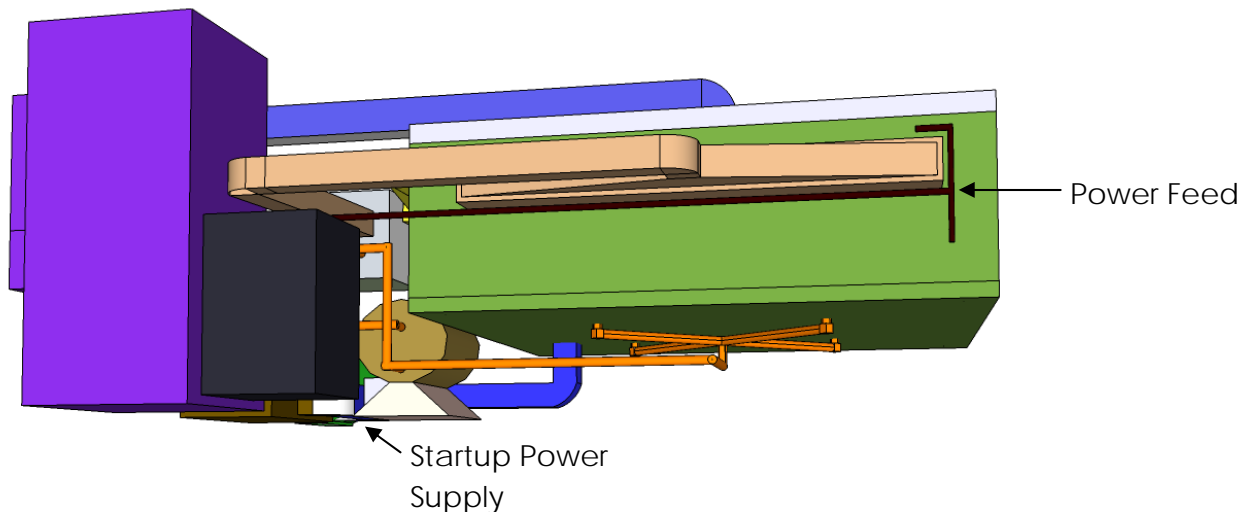


Figure 33: Side View of Control Assembly, Startup Power Supply and Power Feeds

3.4.4.7 Enclosure Assembly

The Ruggedized System Enclosure for the LTA-SOFC Battery Charger (Figure 34 and Figure 35) is designed for field use. The Ambient Air Intake, Air Exhaust, Liquid Fuel Intake, and the User Control Panel are located on a common side of the unit exterior.

The top of the enclosure (removed in Figure 34 to show internal components) is removable for maintenance.

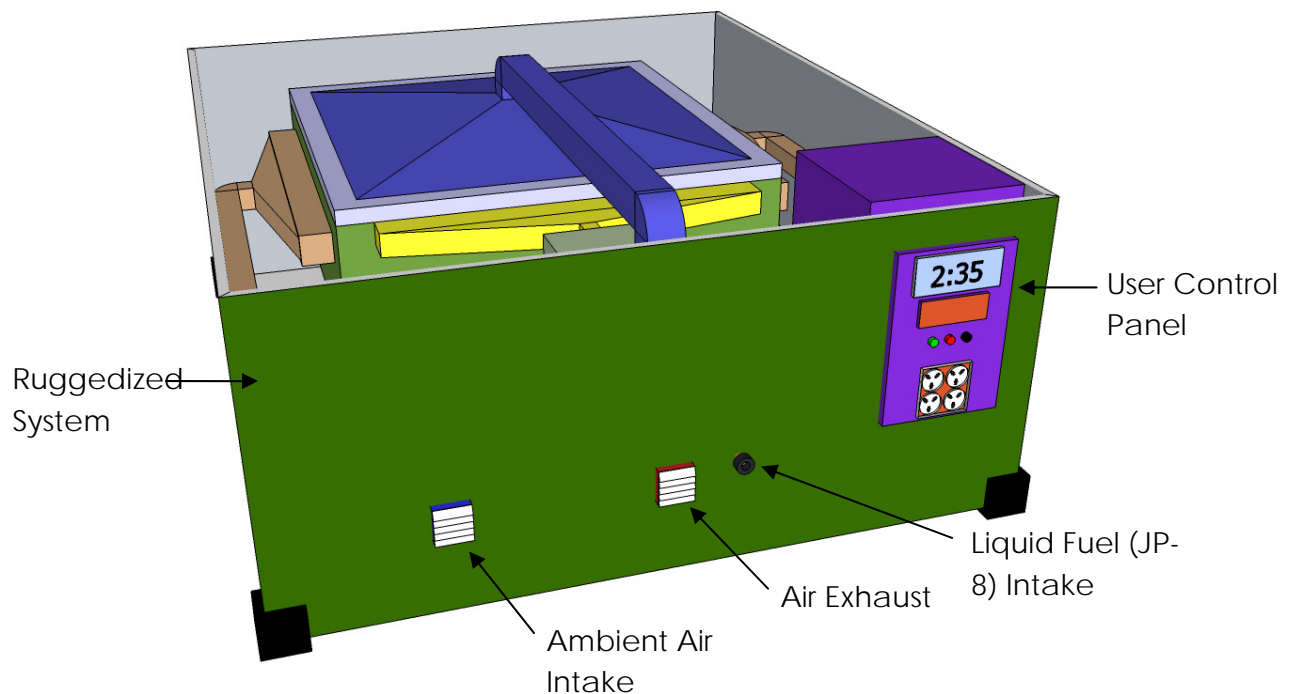


Figure 34: System Casing Without Top Plate

Figure 35 shows the Ruggedized System Enclosure with the Top Plate in place. The Top Plate houses the Battery Charging Adapter Receptacles and the Adapter Receptacle Cover. The Adapter Receptacle Cover is designed to seal the Adapter Receptacles from environmental contamination when the system is not in use. The Battery Charging Adapter Receptacles allow charging of various batteries provided the corresponding battery adapter is provided (i.e., the battery adapter J-6358 shown in Figure 21 would allow the LTA-SOFC Battery Charger to charge BB-2590 Radio Batteries).

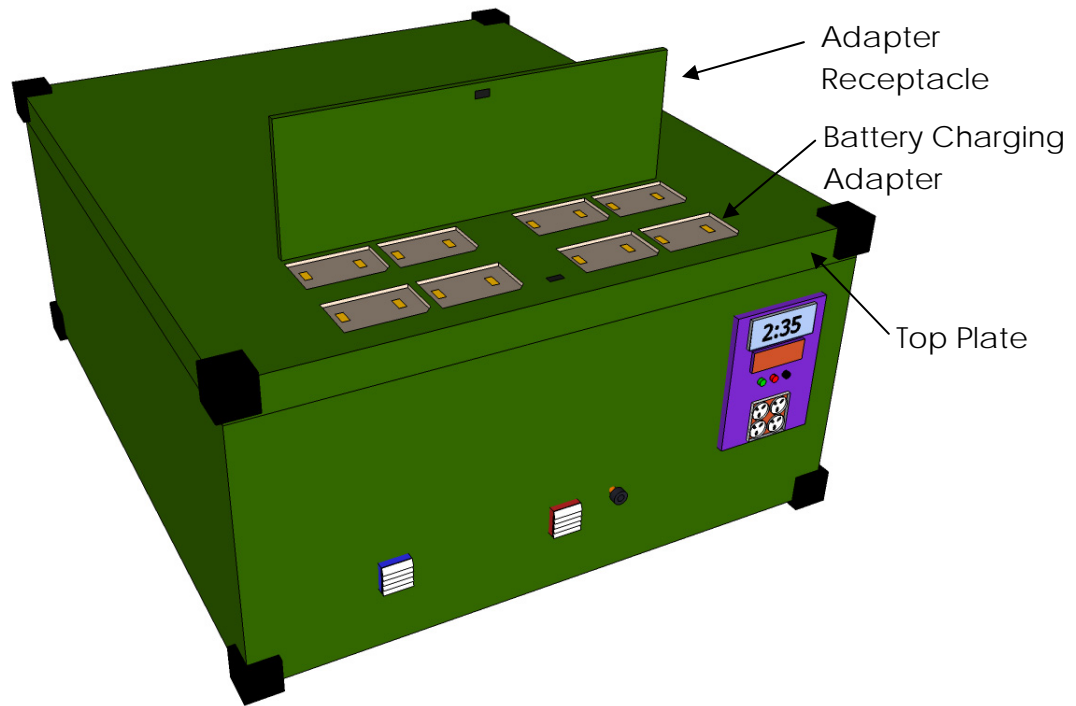


Figure 35: System Enclosure With Top Plate

Future advancements and reduction in cell size will lead to better optimization of system packaging in order to meet volume and weight requirements.

3.4.4.8 Potential Design Trades

The concept design detailed in Section 3.4.4 has various design aspects with potential for further optimization and alternative designs. This section addresses potential future design trades. The design aspects addressed in this section include the method for heating the Hot Subassembly during startup, the method for injecting fuel into the anode chamber of the Hot Subassembly, and the inclusion of an internal battery for system startup.

3.4.4.9 Startup Heating Method

The baseline method for heating up the Hot Subassembly during system startup (resistance heating) has been detailed in Section 3.4.4.2. Two alternative methods could potentially be used to heat the chamber. First, direct heating of the anode chamber could be used to heat the Hot Subassembly during startup. This could be accomplished by directly igniting liquid fuel injected within the Hot Subassembly until operational temperature is attained. The combustion process would need to be controlled to remain fuel-rich, and the Fuel Cell Stack would need to be resilient to the flame temperature of JP-8 without performance degradation. Secondly, indirect heating could be used for startup heating. An adjacent chamber within the Hot

Subassembly could be included in which liquid fuel combustion would occur during startup without directly exposing the Fuel Cell Stack to flame temperatures or oxidizing environment.

The optimal solution would need to meet the following criteria: ability to raise the temperature in the Hot Subassembly to 800°C, moderate energy usage, cause no fuel cell damage, and not introduce unnecessary complexity to the system design.

3.4.4.10 Fuel Injection Approach

The baseline method of injecting fuel into the anode chamber of the Hot Subassembly is detailed in Section 3.4.4.3. The baseline concept design depicts the use of a Fuel Injector Nozzle on a Diffuser Assembly for fuel delivery. An alternative method would be flash fuel vaporization on a hot plate to distribute fuel.

To be optimal, a design would need to evenly distribute the vaporized fuel to all cells, reliably discharge the fuel without clogging, and not introduce unnecessary complexity to the system design.

3.4.4.11 Inclusion of Battery for System Startup

The baseline method for powering the Control Assembly and the baseline Startup Hot Subassembly Heaters is an integrated rechargeable battery connected to the Control Assembly. A potential future consideration takes advantage of external battery power from available military vehicles. Since it is expected that the LTA-SOFC Battery Chargers are likely to be transported by and used in the vicinity of military vehicles, vehicles battery power could be used during system startup. This would decrease the size, weight, and parasitic losses of the LTA-SOFC Battery Charger, but would require compatibility with vehicle batteries and availability of cabling to interface the charger unit with the vehicle battery (i.e., standard battery jumper cables available on most military vehicles). This alternative approach would have external dependencies not present in the baseline system.

4 Summary of Phase 1 results

There is an identified need for a squad-level Direct JP-8 battery charger to support evolving Army mission needs. Additional applications for a Direct JP-8 generator have also been identified. It has been noted that once the Direct JP-8 technology has been developed for squad level battery chargers it can easily scaled for use in many other applications.

The Phase 1 effort of STTR A08-T007 has accomplished the following technical items as defined in Table 3.1.1-1:

1. A range of potential direct oxidation fuel cell anode catalysts have been evaluated. Solid metallic and non metallic anodes and liquid alkaline hydroxides of Na, K and Li were found to be inappropriate due to poisoning from sulfur and carbon. Thermodynamic equilibrium data including the Oxidation ΔG and OCV for a number of p-orbital metals was examined and favorable characteristics were identified for Sn, In, Sb and Bi. Other considerations in the selection of an appropriate liquid metal catalyst include operating temperature, volatility and oxidation kinetics. Based on a ten year history of successful development, the Liquid Tin Anode SOFC technology was selected as the most appropriate liquid metal anode for a near-term battery charger system.
2. The governing anode equations for tin oxidation of carbon, carbon monoxide, hydrogen and hydrocarbons have been defined. Additionally, the equations for direct oxidation of metallic tin (the LTA-SOFC "battery function") and electrical recharging were defined.
3. A detailed electrochemical model (steady state and transient) was developed to simulate the performance of the Liquid Tin Anode (LTA)-Solid Oxide Fuel Cell (SOFC) system. The development of an electrochemical model of the LTA-SOFC Gen3.1 cell has allowed the effect of various physical parameters to be determined. The initial model was one dimensional with simplistic fuel species. The results show that polarization is 22% from the electrolyte, 37% from the anode and 41% from the cathode. Reduction of the electrolyte thickness from 200 μm \rightarrow 50 μm would significantly reduce the electrolyte polarization at current densities above 0.25 A/cm². These results are reflected in another government program for Gen3.2 cells which uses at 75 μm electrolyte. The current exchange density of the anode half reaction was also identified as a potential key limitation to the liquid tin anode. Further refinement of the model and collection of experimental data would verify the effect of current exchange density at the anode. These refinements may allow the anode polarization to be significantly

reduced. The results from the model showed that the material properties of the cathode do not strongly influence cathode polarization. However increasing the cathode air pressure an order of magnitude was shown to significantly reduce the cathode polarization. Further verification with experimental data along with model refinements will lead to the establishment of the major limitations of the LTA-SOFC Gen3.1 cell. These limitations will then be integrated into the system design, i.e. an air blower with higher pressure might be used to reduce the cathode polarization.

4. A system-level analysis and concept design of the 500 Watt battery charger was completed. System requirements were established by identifying the applications of the proposed charger and defining the key needs and requirements of the fuel cell stack assembly. The target family of rechargeable batteries was identified for charging compatibility. Additionally, an existing piece of equipment, the PPS498 Battery Charger, which currently used to charge batteries in the field but requires external power, was examined as part of the design process. A system requirement table was developed (Table 3.4.2-1). Engineering evaluation included:
 - a. A system level flow analysis to determine thermodynamic conditions at key points (Table 3.4.3-1).
 - b. Conceptual drawings of the overall system assembly and 7 key subsystems

Finally, the system-level analysis has identified several potential design trades and alternatives to be evaluated during future detail design activities.

5 Recommended Next Steps

To continue the development of a Direct JP-8 Battery Charger and other DOD requirements, the following steps are recommended:

1. Development and testing of a 250 to 500 Watt LTA-SOFC stack
2. Development of a detailed system design and a breadboard/brassboard 250-500 Watt balance of plant.
3. Development of a system level computer models to establish thermodynamic, dynamic and physical packaging characteristics of a 500 Watt battery charger system.
4. Integration and testing of the stack and brassboard.
5. Further development of the cell-level computer model and validation against test data to further evaluate steady state and transient behavior operating on JP-8.

6 References

1. **S. Karbuz**, *Energy Bulletin*, Feb (2007)
2. **Wolfowitz, P., 2004**, *Department of Defense Directive 4140.25 – DoD Management Policy for Energy Commodities and Related Services*, Department of Defense, Washington, pp.1-10.
3. “Direct Carbonaceous Fuel Conversion including JP-8 in the Gen 3.1 Liquid Tin Anode SOFC”, T. Tao, M. Koslowske, B. McPhee, M. Slaney, L. Bateman, J. Bentley, 2007 Fuel Cell Seminar & Exposition Abstracts 2007, p150-153; “Anode Polarization in Liquid Tin Anode Solid Oxide Fuel Cell”, Thomas Tao, Mike Slaney, Linda Bateman, and Jeff Bentley
ECS Trans. 7, (1) 1389 (2007); “Liquid Tin Anode Solid Oxide Fuel Cell for Direct Carbonaceous Fuel Conversion”, Thomas Tao, Linda Bateman, Jeff Bentley, and Michael Slaney
ECS Trans. 5, (1) 463 (2007); “Liquid Tin Anode SOFC for Direct Fuel Conversion including carbon and JP-8”, T. Tao, M. Slaney, L. Bateman, J. Bentley, 2006 Fuel Cell Seminar Abstracts, p198-201;

“**Direct JP-8 Conversion Using a Liquid Tin Anode Solid Oxide Fuel Cell (LTA-SOFC) for Military Applications**”, W. A. G. McPhee et al., 2008, *Journal of Fuel Cell Science and Technology*, in publication.
4. “**Performance Improvement in Copper Based Direct Oxidation SOFC**”, E. Paz, et al., Abstracts of 2005 Fuel Cell Seminar, Nov 2005, Palm Springs, CA, pp 85-88.
5. “**Development of solid oxide fuel cells for the direct oxidation of hydrocarbon fuels**”, Lu, C., et al., *Solid State Ionics*, Vol 152-153, pp 393-397.
6. **Mayfield, H. T., 1996**, *JP-8 Composition and Variability*, Air Force Materiel Command – Armstrong Laboratory, Tyndall Air Force Base, pp. 1-27.
7. **Robinson, W. A., 1997**, *Petroleum Quality Information Systems Jet Fuel Data (1997)*, Defense Logistics Agency, Fort Belvoir, pp.1-47.
8. “**Draft Fuel Cell Battery Charger System Specification 250–500 W Nominal**”, US Army Research Development and Engineering Command, *Communications-Electronics Research, Development, and Engineering Center (CERDEC)*. 29th September 2004.
9. “An Analytical Model for Solid Oxide Fuel Cells” L. Pisani, G. Murgia, J. Electrochem. Soc., 154, B793 (2007);
10. “A Mathematical Model of a Solid Oxide Fuel Cell” , Norman F. Bessette II, William J. Wepfer, and Jack Winnick, J. Electrochem. Soc. 142 3792 (1995);

11. "A System Level Simulation Model of Sofc Systems for Building Applications" Kwang Ho Lee, and Richard k. Strand, Third National Conference Of IBPSA-USA, Berkeley, California, July 30 – August 1, 2008 (http://www.ibpsa.us/simbuild2008/technical_sessions/SB08-DOC-TS02-2-Lee.pdf)

